2

DOE/ID/12735--T13
2DOE-CCF-D003

DOE/ID/12735--T13

DE91 006537

CERAMIC FABRICATION R&D

Quarterly Technical Progress Report
for
January 1 - March 31, 1990

DISCLAIMER

This report was prepared as an account of work sponsored by an agency of the United States Government. Neither the United States Government nor any agency thereof, nor any of their employees, makes any warranty, express or implied, or assumes any legal liability or responsibility for the accuracy, completeness, or usefulness of any information, apparatus, product, or process disclosed, or represents that its use would not infringe privately owned rights. Reference herein to any specific commercial product, process, or service by trade name, trademark, manufacturer, or otherwise does not necessarily constitute or imply its endorsement, recommendation, or favoring by the United States Government or any agency thereof. The views and opinions of authors expressed herein do not necessarily state or reflect those of the United States Government or any agency thereof.

PREPARED BY

MSE, Inc.
P.O. Box 3767
Butte, Montana 59702

PREPARED FOR

U.S. Department of Energy
Under Contract DE-AC07-88ID12735

Reviewed by: _____
Program Manager

Approved by: _____
General Manager

MASTER

DISTRIBUTION OF THIS DOCUMENT IS UNLIMITED

EXECUTIVE SUMMARY

This project is separated into three tasks. The first task is a design and modeling effort to be carried out by MSE, Inc. The purpose of this task is to develop and analyze designs for various cohesive ceramic fabrication (CCF) components in luding an MHD electrode for strategic defense initiative (SDI) applications and a high stress, low cost, reinforced ceramic component for armor applications. This quarter, the advanced molybdenum disicilide MHD electrode design was essentially completed. Final refinements will be made after molybdenum disilicide processing results are available and the final layer compositions are established. Work involving whisker incorporation was initiated on the high stress component. However, it is unlikely that whiskers will become low cost, so to realize the low cost potential of CCF processing, particulate reinforcement will be pursued. Modeling work will resume once a suitable aluminum oxide/silicon carbide composition is selected that, with the incorporation of sintering aids, can be fired to acceptable densities by pressureless sintering.

Task 2, subcontracted to Applied Technology Laboratories (ATL), is principally directed at establishing a property data base for monolithic and laminated alumina fabricated using the CCF process. This quarter, ATL demonstrated that the CCF process does not compromise the flexure strength of alumina. Strength values substantially equal to those of commercial alumina have been determined. Furthermore, the indistinguishability of the bond in CCF laminated pieces after firing was demonstrated. A matrix experiment designed to identify the critical processing parameters was completed and will be reported on in the next quarterly. High temperature data is also being acquired.

Task 3, subcontracted to Ceramics Binder Systems, Inc., has focused mainly on the production, using the CCF technology, of a four-high stack of planar solid oxide fuel cells. However, work on the planar solid oxide fuel cell was terminated to allow efforts to focus on CCF silicon carbide particulate reinforced alumina and on the development of processing procedures for nonoxide molybdenum disilicide. Preliminary results indicate that achieving high densities in silicon carbide particulate reinforced aluminum oxide will be difficult. Molybdenum disilicide results are encouraging, and it is clear that the CCF process will work with this nonoxide material.

TABLE OF CONTENTS

TABLE OF CONTENTS (cont'd)

1.0 INTRODUCTION

The general goal of the cohesive ceramic fabrication (CCF) research and development project is to develop the CCF process and demonstrate its application to various defense-related systems.

The project has been separated into three individual tasks:

- Task 1 -- Ceramic Component Design and Analysis;
- Task 2 -- Exploratory Development Using the CCF Process; and
- Task 3 -- Ceramic Fabrication and Manufacturing.

2.0 PROJECT DESCRIPTION

2.1 TASK 1 -- CERAMIC COMPONENT DESIGN AND ANALYSIS

The purpose of this task is to develop realistic specifications for various CCF components that will demonstrate the applicability of the CCF process to defense systems, including a magnetohydrodynamic (MHD) electrode for strategic defense initiative (SDI) applications and a high stress, low cost, reinforced ceramic matrix composite with armor applications.

This task is the principal responsibility of MSE, Inc.

2.1.1 Subtask 1A -- MHD Electrode Design and Analysis

The overall thrust of this task is to design a ceramic MHD electrode having advanced characteristics using the unique capabilities of the CCF process.

The initial design will be generated based on input from MHD and materials specialists and design requirements related to SDI applications. The design will then be analyzed using the finite element technique. It is expected that this will be an iterative process involving material changes and dimensional variations.

The end product of this effort will be an electrode design used as the basis for fabricating the electrode in Task 3.

2.1.2 Subtask 1B -- High Stress Component Design and Analysis

In this subtask, a high stress ceramic component with armor applications will be designed and analyzed. Once experiments have shown a feasible composition, the sample piece to be fabricated will be modeled and analyzed with finite element methods.

2.1.3 Subtask 1C -- Project Management

This subtask entails managerial and technical supervision of all Task 1 work as well as oversight and technical and general monitoring of Task 2, which is subcontracted to Applied Technology Laboratories (ATL), a division of Montana Technology Companies, and of Task 3, which is subcontracted to Ceramic Binder Systems, Inc. (CBSi).

This subtask covers reporting technical progress and tracking contract expenditures and work schedules.

2.2 TASK 2 -- EXPLORATORY DEVELOPMENT USING THE CCF PROCESS

This task deals with the generation of a scientific data base for ceramic materials produced using the CCF process. Emphasis is on alumina, but some nonoxide data on molybdenum disilicide ($MoSi_2$) will be generated. Some work on a ceramic matrix composite, most likely the silicon carbide (SiC) particulate alumina matrix system, will also be reported. Data will be obtained to characterize the properties of monolithic and bonded (laminated) ceramic shapes.

2.2.1 Subtask 2A -- Characterization of Starting Materials

Only limited characterization of the starting materials was scheduled because manufacturers's specifications and data are sufficient for most purposes. Some chemical analysis and microstructural analysis were scheduled.

2.2.1.1 Subtask 2A-1 -- Ceramic Process Control Studies

Work conducted during the first quarter showed that aspects of the CCF process were inadequately understood and not reproducibly controlled. Therefore, a series of matrix experiments was designed to identify the causes of process-related defects encountered when thicker parts were attempted. The results will be presented in a later report. Meanwhile, successful production of MIL-STD-1942 test bars was achieved during the second quarter.

2.2.1.2 Subtask 2A-2 -- Characterization of Sintered Ceramic

Sintered ceramic produced by the CCF process is evaluated based on the sintered modulus and modulus of rupture (flexure strength in four-point bending) and on an examination of the microstructure of the sintered material. A thorough examination includes average grain size, grain-size distribution, grain shape, and grain shape distribution. Defect distributions are also significant; these include crack lengths, widths, and distributions and void (pore) sizes, shapes, and distributions.

Grain size is important because strength is usually inversely proportional to the square root of the grain diameter. Hence, a fine and uniform grain size results in high strength. But high strength also requires minimization of porosity, since pores and voids act as stress concentrators, which may substantially reduce strength.

Characterization of sintered microstructure for this project relies primarily upon scanning electron microscopy examination because of the fine grain size and small pore size in sintered ceramic.

2.2.2 Subtask 2B -- Mechanical Test Methods

Mechanical testing is necessary to secure quantitative information on the strength of ceramics produced by the CCF process. Monolithic ceramic will be tested to provide data for comparison with regular commercial ceramic and also to establish a baseline against which the strength of laminated (bonded) parts can be assessed. Testing to MIL-STD-1942 for flexure strength is planned in addition to some other testing conducted to ascertain fracture toughness values. The diametral compression test will be used to develop information about the tensile strength of the CCF bond.

2.2.2.1 Subtask 2B-1 -- Flexural Testing to MIL-STD-1942

Four-point bend testing to MIL-STD-1942 is widely applied and accepted. The standard details well-defined surface preparation, which is important for providing valid comparison among materials. Specimens will be sent to experienced outside vendors for preparation. In-house, as-fired specimens will be extensively tested as part of the exploratory and development effort.

Most ambient testing will be conducted in-house, and elevated temperature testing will be conducted by a properly equipped, experienced vendor.

2.2.2.2 Subtask 2B-2 -- Short Rod Fracture Toughness Testing

ATL is equipped with a Terratek Fractometer I System 4201 test apparatus. This will test fracture toughness according to ASTM Standard B-771, Standard Test Method for Short Rod Fracture Toughness of Cemented Carbides. An advantage of this test is that specimens can be readily produced in-house. The method appears to offer a reproducible way to obtain reportable fracture toughness data for ceramic materials.

2.2.2.3 Subtask 2B-3 -- Fracture Testing of Joints

A standard or widely accepted test for fracture toughness testing of ceramic material bonds is not available. Hence, available fracture toughness test methods as they apply to bonds in laminated ceramic items will be evaluated. It is possible that the short rod test in Subtask 2B-2 will be best, but alternatives will be explored.

2.2.2.4 Subtask 2B-4 -- Diametral Compression Test

The diametral compression test appears to have the potential benefit of providing tensile strength information because fractures can be initiated internally as a result of the stress distribution that prevails in the specimen used in this test. Furthermore, the cylindrical specimens necessary can be core-drilled readily from fired ceramic pieces. In addition, it should be possible to orient the bonded region in laminated pieces along a diametral plane and normal to the test platens. Accordingly, this test method is under serious consideration.

2.2.2.5 Subtask 2B-5 -- Microindentation Fracture Toughness Test

In brittle materials, indentation tests for hardness measurements are apt to be in error due to cracks generated by the indentor. These cracks may be useful in assessing the fracture toughness of the material; extensive literature studies on the applicability of this test for assessing the fracture toughness of joints made with the CCF process exist. It is necessary to determine whether the fracture toughness values determined by the microindentation method are comparable with those obtained from the short rod method. If so, microindentation testing will be a simpler and faster way to assess fracture toughness of joints and laminated specimens.

2.2.3 Subtask 2C -- Development of Ceramic Specimens for Laminated Bond Testing

The proprietary CCF process imparts a unique pliability to otherwise nonplastic, green ceramic powders. This pliability allows complex shapes to be fabricated without extremely expensive shaping equipment and tooling. Because the CCF process is sufficiently novel, it is imperative to establish that the CCF process can yield high-quality sintered alumina ceramic material with properties equivalent to those of alumina obtained with the traditional ceramic shaping processes (dry pressing, extrusion, and slip casting).

Since the CCF process differs substantially from the more traditional techniques, it is also necessary to establish the optimum processing procedure so the process is compatible with lamination bonding. However, the lamination operation has to be optimized and detailed procedures established.

Lamination bond quality can be determined by comparing the modulus of rupture of monolithic samples with those of lamination bonded samples. If statistically significant differences occur between monolithic and laminated specimens and the laminated specimens are weaker, then the bond interface is inherently weak, and process modifications may be needed to increase the bond strength.

2.2.4 Subtask 2D -- Ceramic Matrix Composites Using the CCF Process

Superior engineering properties and performance can be obtained by combining two or more materials to form a composite. Desirable mechanical properties (strength and toughness) are possible with fiber reinforcement (such as fiberglass reinforced plastics). Composites with potential for high temperature, high stress applications include: ceramic fiber in a ceramic matrix, ceramic fiber in a metal matrix, and metal fiber in a ceramic matrix.

Fabricating ceramic matrix composites is difficult because fiber reinforcement interferes with particle packing and compaction. In addition, the fibers often inhibit densification so sintering becomes difficult. Therefore, "high tech" composites are often extremely expensive because fibers are costly, and the composite often requires hot pressing, hot forging, or some other high cost fabrication technique.

The CCF process has promise for improving composite fabrication because the pliability of the plasticized ceramic matrix allows complex shapes. Considerable process development will be required to incorporate selected fibers and attain high sintered densities.

The system chosen for study is silicon carbide whiskers/fibers in an alumina matrix. Considerable experience with this system is reported in literature but mostly with hot-pressed material. Since the CCF process uses pressureless sintering, initial efforts will be directed at selecting process variables such as sintering aids, volume percent of whiskers, etc. to yield acceptable densities. A composition and process procedure will then be selected, and the processed ceramic will be tested to secure a data base of mechanical property and microstructural information.

2.3 TASK 3 -- CERAMIC FABRICATION AND MANUFACTURING

The overall goal of CBSi is to fabricate complex ceramic components to demonstrate the applicability of CCF technology for defense purposes. The CCF process has the potential to extend the number and complexity of ceramic components available to the government. The goal of the proposed work is to produce complex ceramic shapes that have near-term applicability to Department of Defense requirements.

CBSi will produce three complex ceramic components during the course of this contract. The first component is a model of a solid oxide fuel cell, the second is an advanced concept model MHD electrode, and the third is a curved shape with armor applications.

2.3.1 Subtask 3A -- Solid Oxide Fuel Cell

The solid oxide fuel cell (SOFC) is a planar fuel cell design that allows a higher density membrane area than other SOFC designs. During the first quarter, a complex, multilayer, stabilized zirconia fuel cell model was fabricated, and good progress was made. However, shape, dimensional, and tearing problems were encountered when multilayer cell stacks were attempted. After the second review meeting on January 17, 1990, development work on the SOFC was halted so efforts could be concentrated on the other two subtasks. The work conducted to this point will be reported, and a demonstration single cell will be deliverable.

2.3.2 Subtask 3B -- MHD Electrode Fabrication

The second component to be fabricated is an advanced MHD ceramic electrode. The electrode was designed by MSE with collaboration from CBSi during the first phase of the project. The candidate material selected was molybdenum disilicide ($MoSi_2$). Modeling and analysis of the proposed layered structure with compositional grading to meet the requirements of the specifications set out in the second quarterly report are being carried out by MSE. As $MoSi_2$ is a covalently bonded, nonoxide material, it provides an excellent opportunity to demonstrate the applicability of the CCF technology to nonoxide ceramics. CBSi will fabricate the design after the composition and dimensions are refined.

2.3.3 Subtask 3C -- High Stress Component Fabrication

The third component to be fabricated is a ceramic component that experiences high stress, thermal or mechanical, while in service. An armor application has been selected since it enables the demonstration of low cost fabrication of doubly curved shapes using the CCF process. A ceramic matrix composite based on silicon carbide (SiC) in alumina will be produced. A data base will be generated and ballistic test plates will be fabricated. Initially, SiC whiskers were procured; however, given the emphasis on low cost fabrication, efforts will be concentrated on SiC particulate reinforcement. MSE will analyze the design, and CBSi will fabricate the component.

3.0 PROJECT STATUS

3.1 TASK 1 -- CERAMIC COMPONENT DESIGN AND ANALYSIS

In Subtask 1A, modeling and analysis of the layered, graded $MoSi_2$ electrode was essentially completed. A few final refinements are likely. However, they will not be made until CBSi experimental results are available, which will allow the final compositional grading and layering to be established.

In Subtask 1B, the results of the CBSi experiments are needed to fix the composition of the ceramic matrix composite to be modeled and analyzed.

3.1.1 Subtask 1A -- MHD Electrode Design and Analysis

Molybdenum disilicide ($MoSi_2$) was chosen as the electrode material; however, finite element analysis indicated thermally induced stress of the same magnitude as the nominal tensile strength of the material would be generated during startup. Silica glass was selected from several potential grading materials to be incorporated as a second phase to lower the thermal expansion coefficient of the $MoSi_2$. By creating layers having different percentages of silica glass, the calculated thermal stresses could be brought under the nominal tensile strength of the pure $MoSi_2$. The CCF process is ideally suited to fabricating an electrode structure composed of layers having different compositions.

Figure 1 shows the calculated temperature distribution as a function of time after startup. Steady state is reached approximately 50 seconds after startup. The maximum tensile stress, approximately 180 MPa, is developed between 3 and 5 seconds after startup as shown in Figure 2. The nominal strength of $MoSi_2$ is approximately 196 MPa. The layered design to accommodate this situation is shown in Figure 3, which shows that grading with up to 15 volume percent of silicon dioxide (SiO_2) glass in the middle layers is needed. The calculated stresses for the steady-state condition are shown in Figure 4. The transient stress conditions in the X-direction are shown, for 1 to 5 seconds after startup, in Figure 5. This shows a high tensile stress region moves down through the electrode from the surface during the heating phase.

During March, additional analysis was performed to investigate the amount of Joule heating dissipated in the electrode under normal operating conditions where current density of 8 A/cm^2 is assumed. The electrical resistivity of Kanthal Super 33 ($MoSi_2$), taken from the Kanthal Handbook, is rearranged in curvefit form as $r = (0.22+T\times((4-0.22)/1{,}800))\times10^{-4}$ where r is the electrical resistivity in $\Omega\cdot cm$ and T is temperature in degrees celsius. Silica glass has near zero electrical conductivity and is incorporated as a second phase in $MoSi_2$. The rule of mixtures is used to calculate the electrical conductivity of the $MoSi_2/SiO_2$ graded composition from which the Joule heating dissipated is calculated from

$$Q_{joule} = J^2/\sigma$$

where Q_{joule} is the energy dissipated through Joule heating, J is current density, and σ is the calculated electrical conductivity.

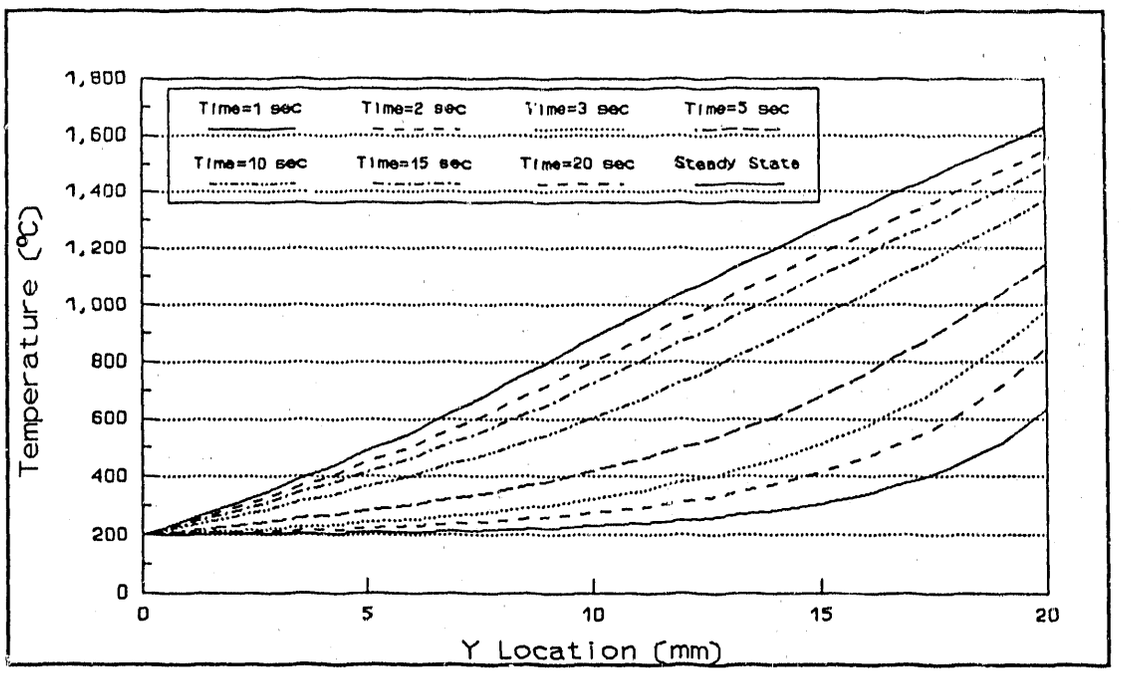

FIGURE 1 -- TEMPERATURE DISTRIBUTION

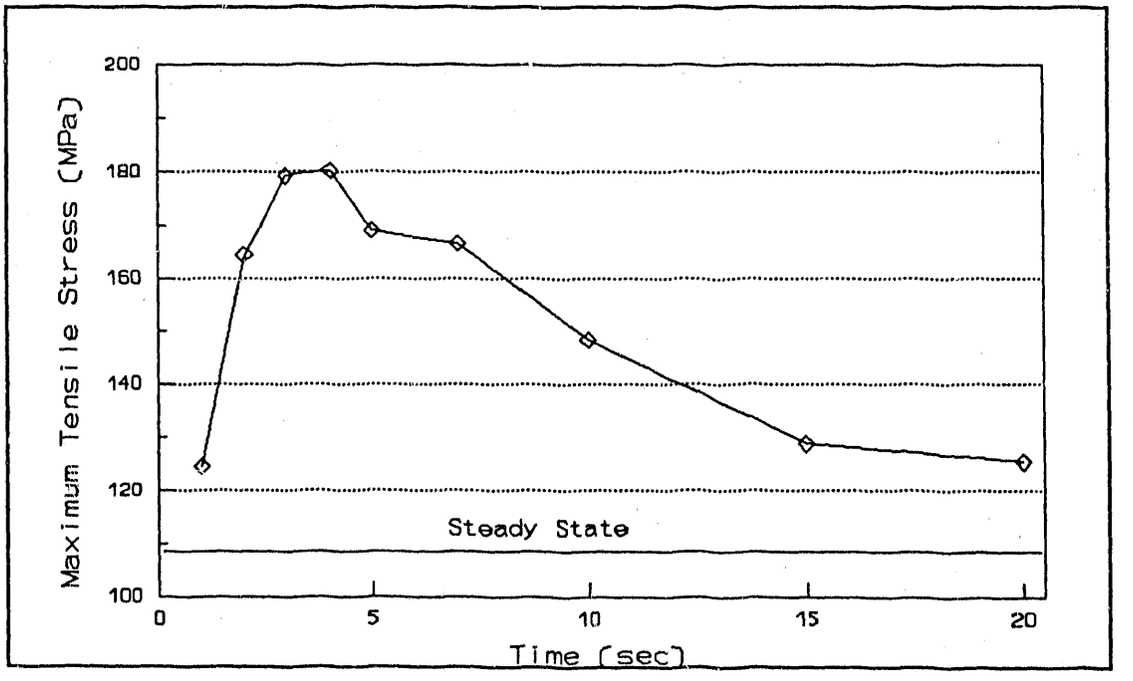

FIGURE 2 -- MAXIMUM TENSILE STRESS

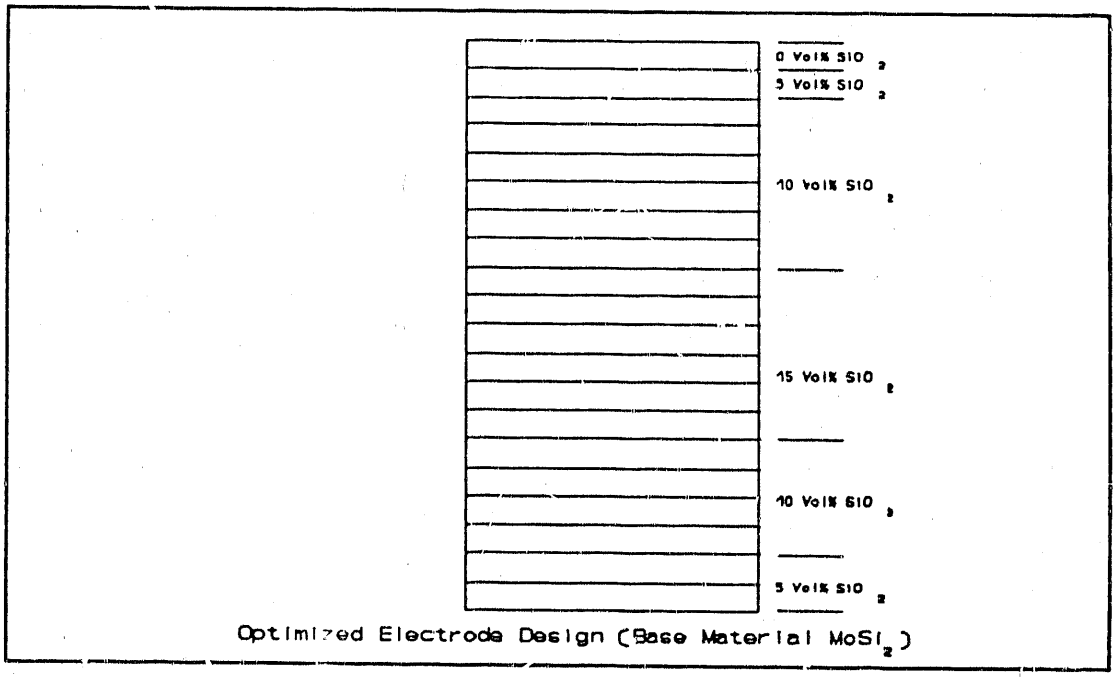

FIGURE 3 -- MHD ELECTRODE DESIGN

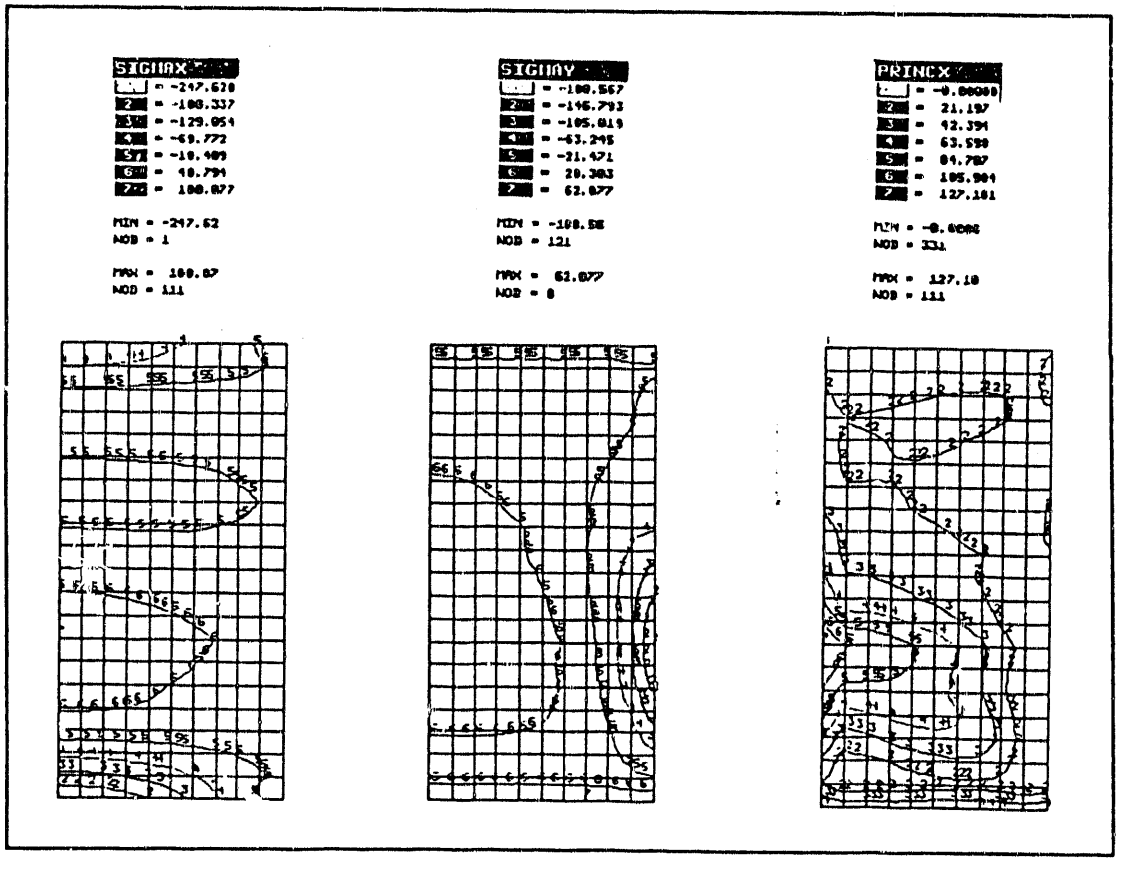

FIGURE 4 -- σ DISTRIBUTION IN $MoSi_2$ SYSTEM (STEADY STATE)

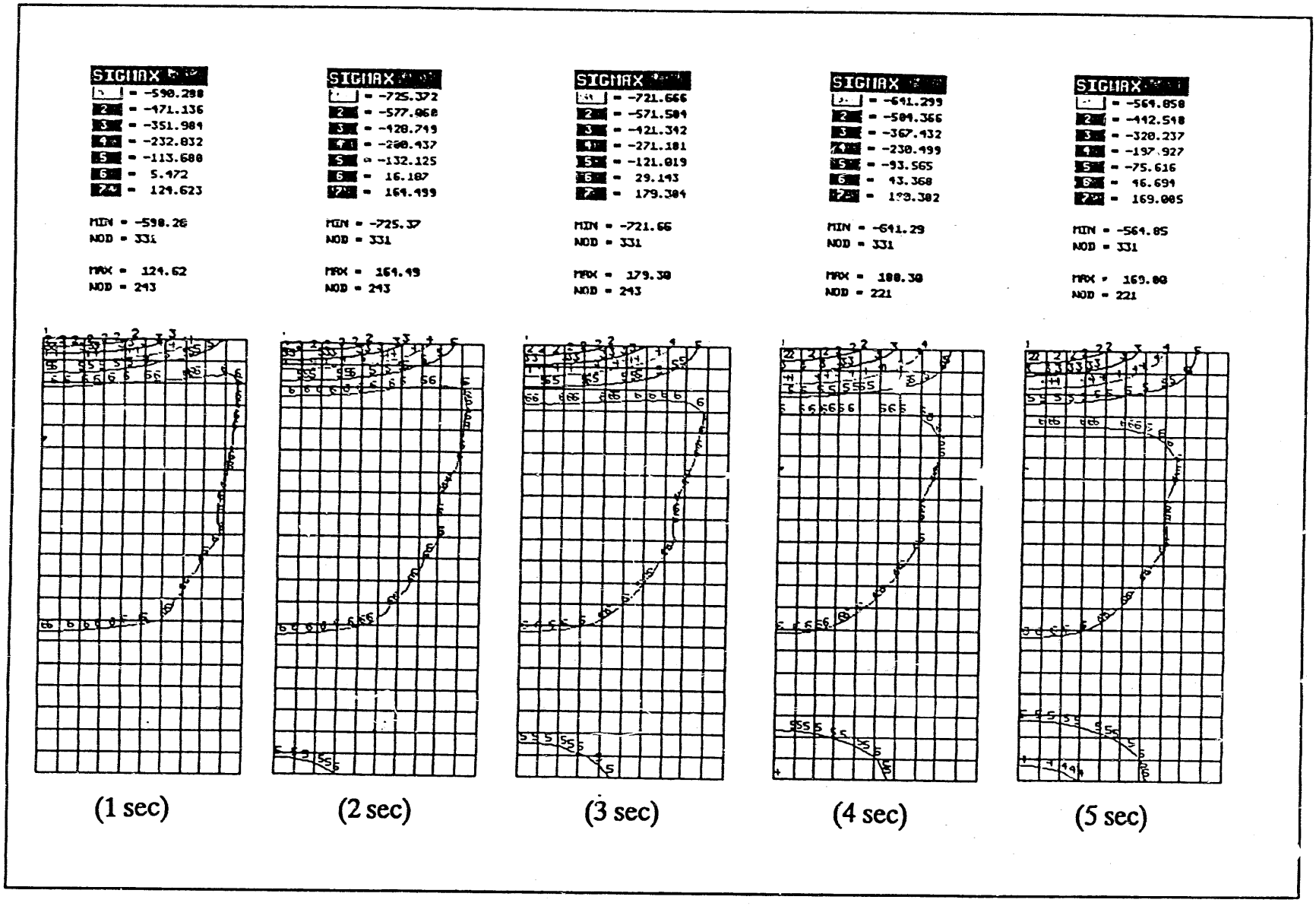

FIGURE 5 -- σ_x DISTRIBUTION IN $MoSi_2$ SYSTEM (TRANSIENT ANALYSIS)

Figure 6 shows the electrical conductivity and Joule heating distribution in the graded ceramic electrode described in Figure 3. The results indicate the Joule heating dissipated in the electrode under normal operating conditions is negligible.

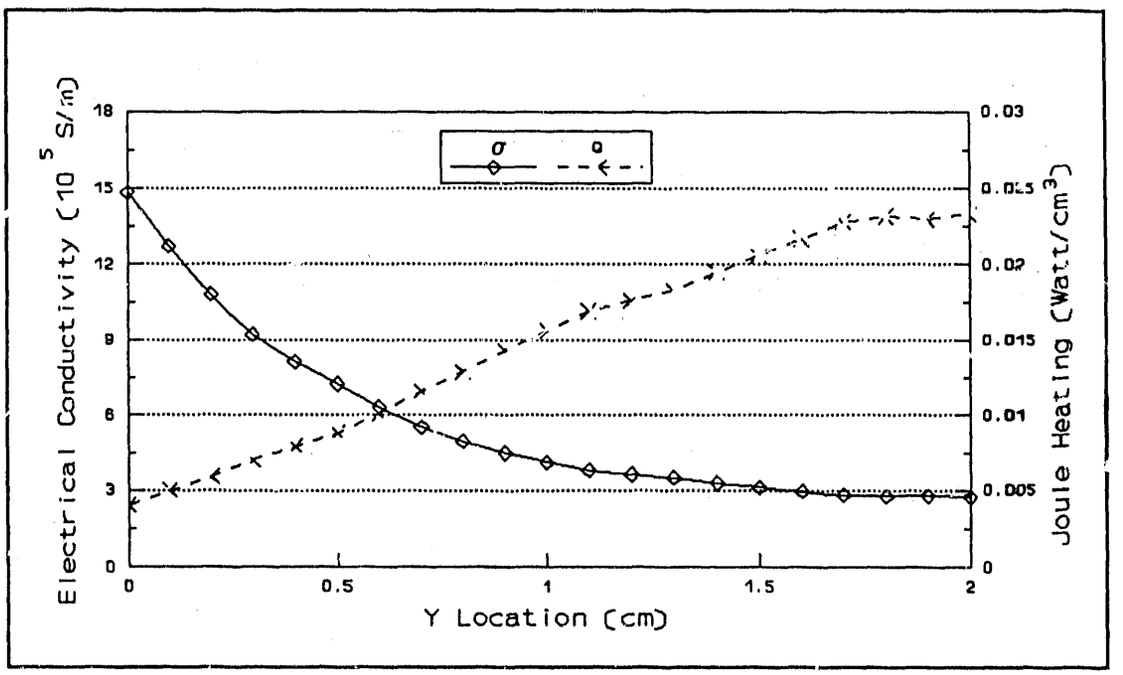

FIGURE 6 -- ELECTRICAL CONDUCTIVITY AND JOULE HEATING DISTRIBUTION

3.1.2 Subtask 1B -- High Stress Component Design and Analysis

The emphasis in this subtask is to demonstrate the potentially low cost fabrication of complex shapes with armor applications. Because of the low cost objective, the initial thrust to incorporate whiskers has been set aside because ceramic whiskers are high cost materials, and it is unlikely that any material containing useful quantities of whiskers will become low cost. A small quantity of alumina containing SiC whiskers was purchased by CBSi, and some experiments were done. These are reported by CBSi. Currently, work is directed at incorporating SiC particulates. The literature shows that current armor work involves materials such as titanium diboride (TiB_2), boron carbide (B_4C), and other very hard, low density materials. Although alumina has a higher density than TiB_2 or B_4C, it is much less expensive. Therefore, alumina was selected as the base material for this task to keep with the low cost objective.

Particulate SiC is not an expensive material. One of the attributes of the CCF process is the ease with which complex curvature can be fabricated; this is presumed to have considerable merit for armor shapes. Thus, a demonstration piece with double curvature will be produced.

However, the CCF process normally employs pressureless sintering, so achieving high sintered densities can be a problem. When a second, inert, dense phase is incorporated, it becomes even more difficult to achieve high densities using pressureless sintering because shrinkage is impeded by the second phase. Hot pressing or hot isostatic pressing is normally adopted to solve this difficulty, but these methods are expensive, slow processes, and even hot isostatic pressing is restricted to relatively simple shapes. Consequently, CBSi proposes to address this problem by using sintering aids to significantly lower the sintering temperature so more effective densification can take place at the usual sintering temperature. CBSi is presently conducting experiments with sintering aids in CCF alumina/particulate SiC and will select a composition with which to proceed. Modeling and analysis of the proposed shapes can proceed after the composition is selected. ATL will generate a mechanical properties data base for the chosen composition.

3.2 TASK 2 -- EXPLORATORY DEVELOPMENT USING THE CCF PROCESS

3.2.1 Subtask 2A -- Characterization of Starting Materials

3.2.1.1 Subtask 2A-1 -- Ceramic Process Control Studies

Since the ceramic process control studies were initiated in August 1989, significant changes and refinements have been made in the CCF process to improve quality and consistency. These changes are shown in Figure 7, which compares the old and current versions of the CCF process employed by ATL.

3.2.1.1.1 Mixing

Better homogeneity has been attained by fiber spinning. The mix of organics, binders and solvents, and high purity alumina powder is ball milled with sufficient acetone to produce a pourable slurry. The slurry is then poured into a cup in the center of the spinner where it flows onto a nozzle that spins, thereby whirling the slurry centrifugally. The fluid strings (threads) lose acetone and collect as fibers on the shell of the spinning chamber. The fibers, resembling cotton, are collected and compacted into a slug in an extruder to ensure deairing.

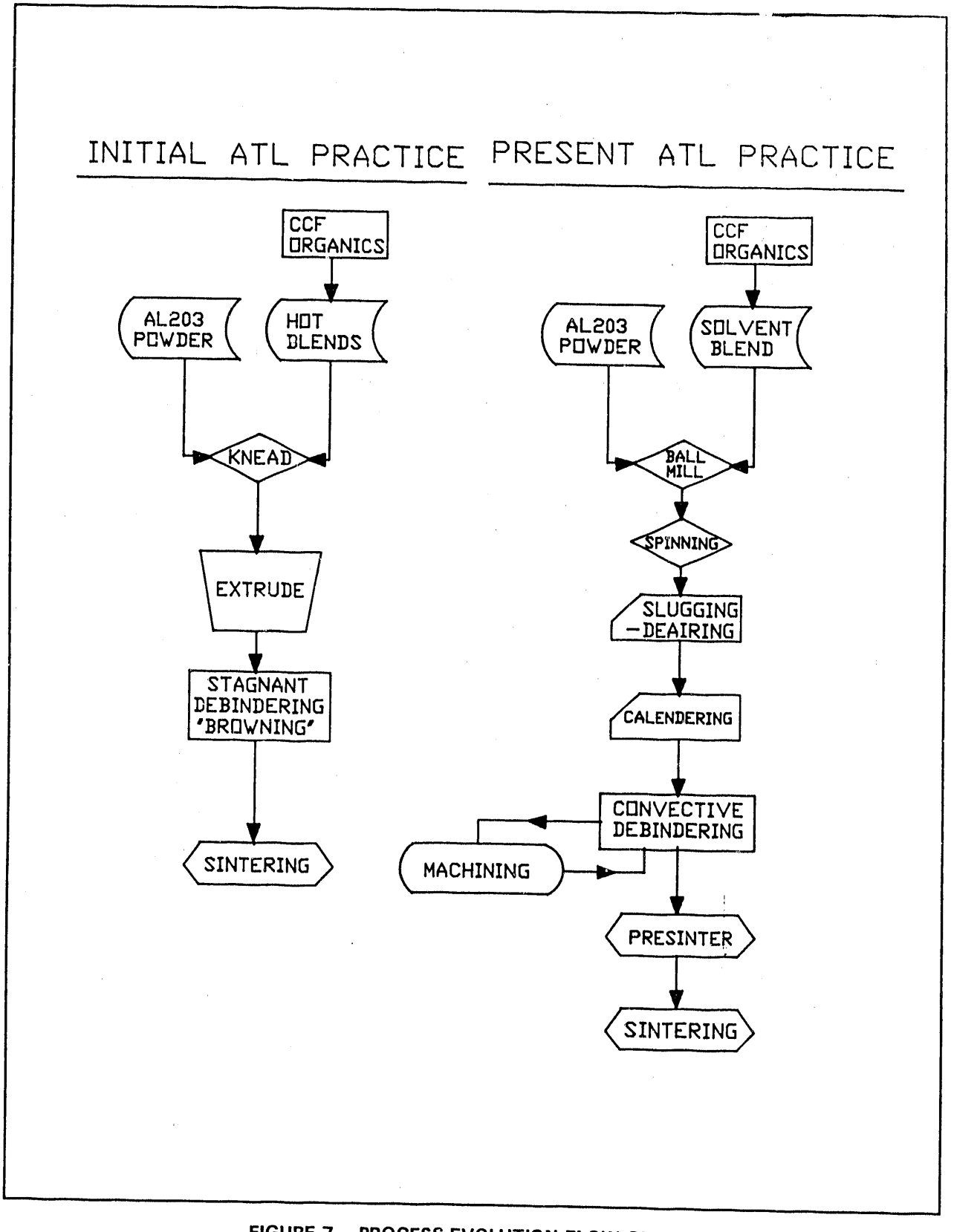

FIGURE 7 -- PROCESS EVOLUTION FLOW CHART

Fiber structure is shown in Figure 8. The fibers are ribbon-like with aspect ratios greater than 20:1 and no evidence of shot (clumps of tangled fibers). The width/thickness ratio seems to be about 5:1, giving very approximate dimensions of 600 by 25 by 5 μm. The fibers seem to be entangled in a configuration analogous to steel wool. Strength of the spun fibers is sufficient so they will not disintegrate before they can be sintered to high density.

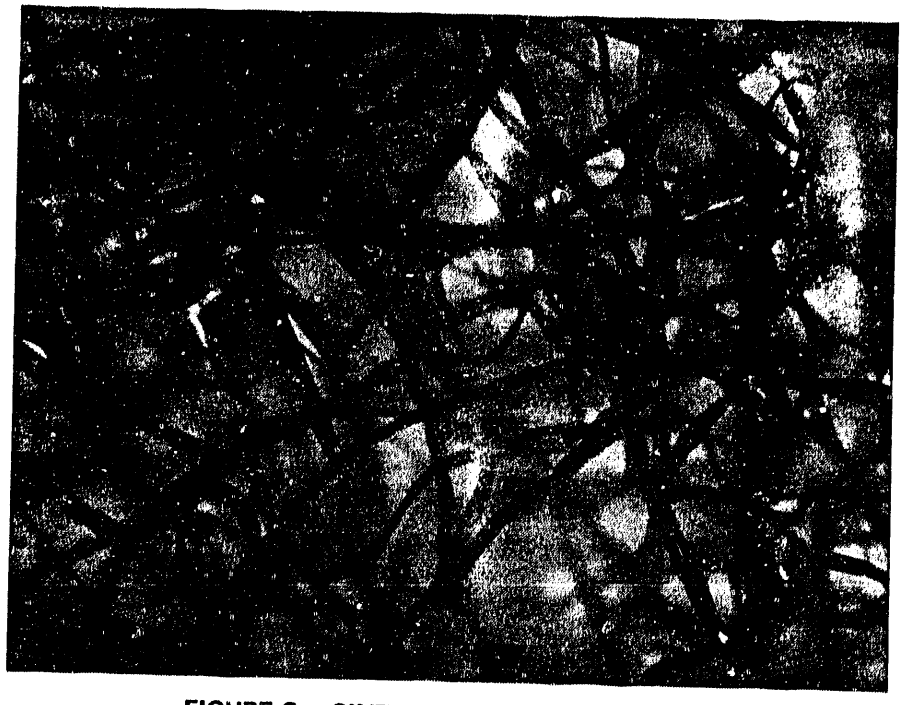

FIGURE 8 -- SINTERED CCF PROCESS FIBERS

The fibers are composed of the fine alumina powder (less than 0.5 μm) dispersed in the CCF organic slurry; the powders (about 50 volume percent) act as a filler for the organic binder. The slurry is slung out by the spinning disc, thereby losing acetone rapidly. As the slurry loses acetone, the viscosity increases greatly so the slurry becomes fibrous instead of forming droplets. As the fibers are whirled outward, they form a ribbon-type structure instead of a smooth, circular cross section fiber. The ribbons are not flat but fairly flat to incompletely circular.

When the organic is removed by browning, only the ceramic powder remains, held together by very weak forces. The powder sinters together and shrinks above 1,100 °C producing a ceramic in the shape of the original fiber. The microstructure of the fiber-shaped ceramic is typically equiaxed grains approximately 3 μm in diameter. The grain size and microstructure are not determined by the original shape of the fiber. Ultimate grain size and shape will be produced by sintering time and temperature, although loose packing can retard grain growth to some extent.

The intended function of fiber spinning is acetone removal; the acetone is added for ball milling to improve homogenization of the CCF organics with the fine, high purity alumina powder. It is essential to coat each particle of alumina uniformly to avoid clumps and clods of uncoated powder. The combination of ball milling, fiber spinning, and slug compaction has improved the quality and consistency of the CCF-processed ceramic specimens.

The CCF-processed fibers are not likely to disintegrate during compaction due to the high strength of the CCF binder system. These fibers are probably squeezed together during calendering or extrusion. Good green (compacted) densities and good sintered densities are obtained, so it appears that the unique pliability of the CCF materials ensures tight packing even with unfavorable structure precursors (such as ribbons).

This raises questions as to the effects of mixing techniques (such as muller mixing, calendering, sigma mixing, etc.) on the fabrication structure. There may also be some merit in adjusting the fiber spinning process to change the fiber structure so circular or other fiber cross sections are produced. It is encouraging that fibers can be formed and sintered without blobs, clusters, shot, or other heterogeneities.

3.2.1.1.2 Debindering

The quality of sheets and plates was improved substantially by emphasizing convection debindering and avoiding radiant heating, especially for thick samples. This convection process involves a programmed flow of heated air over the surfaces of the parts, taking care to place the parts on grills or rails so the top and bottom surfaces are exposed to the flowing hot air. The temperature is programmed to rise to 230 °C on a schedule dependent upon the thickness. Convection heating has resulted in substantially less cracking and warping of samples.

A second measure, which has improved overall quality of CCF-processed ceramics, is a presinter operation. The browning (debindering) step reduces the organic content to approximately 1 to 4 percent of the alumina powder. A lower organic content results in a weak, brittle material that cannot be safely transferred to the sintering furnace without mechanical damage. The residual organic needed for strength often results in blisters, cracks, and laminations, due to the relatively rapid heating rate in the furnace.

A presinter operation that raises the temperature to 1,000 °C in 8 hours removes the organics remaining from browning without creating processing flaws. At this temperature, some sintering is initiated, which strengthens the samples. However, less than 1 percent shrinkage occurs so there is no dimensional distortion. This presintering step improves the use of the furnace since long sintering schedules are required to safely remove the residual organic and sinter to final density in a single furnace cycle.

ATL has been using a Kanthal-wound, 240-V Paragon pottery kiln with a capacity of 2.5 ft^3 for the presintering operation. This is controlled by a Model CN2010 Omega controller, which switches two 25-A solid state relays. Considerable difficulty with arcing and premature turnoff has occurred between 500 and 800 °C. This problem has been solved by cooling the controller with a fan.

3.2.1.1.3 Sintering

A heat balance problem is encountered with the sintering furnace. This furnace has excellent lightweight thermal insulation, which provides low heat leakage through the walls and also low heat storage. The quality of this insulation reduces power requirements and allows rapid heating and cooling. However, the heating is more load sensitive since it takes longer to heat a full load of samples and relatively heavy refractory plates. This is a lesser problem for old style furnaces with heavy bricks since the ratio of furnace lining mass to furnace load (samples and plates) is large. When the sintering furnace is fully loaded, this ratio is relatively small when compared to a lightweight load. In the case of full loading, samples in the center of the furnace will be substantially lower in temperature than the furnace walls until the mass reaches equilibrium with the walls. The thermocouple in the furnace primarily responds to the wall temperature, resulting in a sample temperature that substantially lags the programmed temperature and time.

This makes it difficult to get equivalent sintering since it is necessary to increase programmed temperature and lengthen the time at temperature to compensate for this thermal lag. If the program is not changed, sintered densities will be low (hence low strength). If the program is changed to raise the set point temperature and/or lengthen the hold time, substantial grain growth (hence lower strength) will occur unless the increase in time and temperature are carefully balanced. This problem is being dealt with by using a more standardized mass (more constant mass of plates) per cycle. Lower mass firing plates using compacted CCF fibers are also being fabricated.

3.2.1.1.4 Statistical Process Control Matrix Design

As an integral part of the ceramic control studies, a statistical experimental design plan was formulated to identify critical processing parameters as described in the previous quarterly report (Section 3.2.1.1, Subtask 2A-1). This experimental matrix is detailed in Tables 1 and 2. The 16 selected experimental runs have been formulated, fabricated, and sintered. Results of the

TABLE 1 -- EXPERIMENTAL DESIGN VARIABLES FOR STATISTICAL MATRIX*

PROCESS VARIABLES	LEVEL 1 (+)	LEVEL 2 (-)
Mixing Methods	Spinning	Sigma Mixing
Fabrication Method	Extrusion	Calendering
Alumina Powder Type	Alcoa A16SG	Reynolds RC-HP-DBM +0.05% MgO
Binder Content	Standard Level	Half Standard Level
Dispersant Content	Standard Level +3% Additional	Standard Amount
Browning Cycle	56 Hours	27 Hours
Browning Airflow Rate	High	Low

*"Design of Experiments Course," Volume 5, J. S. Hunter, Westinghouse

evaluation of this matrix will be presented in the April monthly status report. Evaluation criteria include sintered density, warping, cracking, blisters, and delaminations.

3.2.1.2 Subtask 2A-2 -- Characterization of Sintered Ceramic

Sawing, grinding, and polishing damage the surface layers of the ceramic specimens, thereby masking the optical or scanning electron microscopy examination of grain size, grain-size distribution, and grain structure. The extreme corrosion resistance of dense sintered alumina makes it difficult and tedious to suitably etch. ATL has found that thermal etching a ground and polished sample to 1,550 °C for 30 minutes (about 100 °C below the usual sintering temperature) anneals out the damage without causing grain growth. This produces satisfactory etching and delineation of microstructural features.

TABLE 2 -- STATISTICAL EXPERIMENT PLAN PROCESS VARIABLE[1]

RUN	A	B	C	D	E	F	G*
1	+	+	+	+	+	+	+
2	-	+	+	-	-	+	-
3	+	-	+	-	+	-	-
4	-	-	+	+	-	-	+
5	+	+	-	+	-	-	-
6	-	+	-	-	+	-	+
7	+	-	-	-	-	+	+
8	-	-	-	+	+	+	-
9	+	+	+	-	-	-	+
10	-	+	+	+	+	-	-
11	+	-	+	+	-	+	-
12	-	-	+	-	+	+	+
13	+	+	-	-	+	+	-
14	-	+	-	+	-	+	+
15	+	-	-	+	+	-	+
16	-	-	-	-	-	-	-

[1]"Design of Experiments Course," Volume 5, J. S. Hunter, Westinghouse
*For explanation of + and -, refer to Levels 1 and 2 of Table 1.

3.2.2 Subtask 2B -- Mechanical Test Methods

3.2.2.1 Subtask 2B-1 -- Flexural Testing to MIL-STD-1942

Six plates were fabricated from RC-HP-DBM powder containing 0.05 percent magnesium oxide (MgO) by calendering and then sintered at 1,600 °C for 4 hours. These plates (lot 61) were sent to Chand-Kare Corporation for cutting and grinding into MIL-STD-1942B bars; 38 test bars were then fractured in four-point bending with an Instron tester.

Another batch of plates was calendered and sintered from A16SG powder (lot 68) and sent to Chand-Kare for cutting per MIL-STD-1942B. These bars were divided into three groups. One part of Lot 68 (13 bars) was tested in-house while the remainder were sent to the University of Utah for room temperature (35 bars) and 1,000 °C modulus of rupture measurements (23 bars).

The processing history of all the flexure tested lots is summarized in Table 3. ATL has now demonstrated that good alumina ceramics can be made from Reynolds RC-HP-DBM +0.05 percent MgO powder and from Alcoa A16SG powder. It has also been shown that in-house bars are close in strength to MIL-STD-1942B bars, which means that the dominant contributors to strength are: high sintered density; a small, uniform grain size; and the absence of cracks and surface flaws.

The four-point bend test fixture and the testing procedure employed by ATL appear to be suitable since the flexure strength at room temperature obtained by ATL correlates closely with that found by the University of Utah. Some difference exists in the Weibull modulus (and hence standard deviation), but the sample sizes were different so a higher modulus for the Utah sample is not unreasonable.

The correlation between flexure strength (modulus of rupture) and average grain diameter is indicated in Figure 9. The flexure strength of ceramics follows an inverse square root of average grain-size relationship. This relationship was developed for metals by Petch[1] and was extended to ceramics by Carniglia[2]. The Petch equation is followed for small grain sizes under 50 μm, but larger grained ceramics conform to Knudsen's equation:

$$f = k_1(D)^{-1/2} \quad \text{(Knudsen)}$$

compared to:

$$f = \sigma_i + k_2(D)^{-1/2} \quad \text{(Petch)}$$

where:

f is the average fracture stress
D is the average grain size
σ_i is friction stress (stress to where fracture crystal)
k and k_2 are empirical constants

TABLE 3 -- PROCESSING HISTORY OF MOR TEST GROUPS (FOUR-POINT FLEXURE)

LOT	DATE TESTED	NUMBER OF SAMPLES	ALUMINA POWDER	FABRICATE METHOD	AVERAGE SINTERED DENSITY (%)	AVERAGE MOR (ksi)	STANDARD DEVIATION (%)	WEIBULL MODULUS	AVERAGE GRAIN SIZE (microns)
--	August	72	A16SG	Calendered	93.4	14.11	35.1	3.45	--
--	November	8	A16SG	Extruded	95.8	48.71	19.5	3.89	--
--	December	21	RC-HP-DBM no MgO	Extruded	98.1	35.17	17.1	5.50	25[4]
61	February	38	RC-HP-DBM with 0.05 MgO	Calendered MIL-STD-1942B	97.6	53.33	18.0	5.63	6
68	March	13	A16SG	Calendered MIL-STD-1942B	95.0	42.31	13.5	5.65	15[1]
68	March	35	A16SG	Calendered MIL-STD-1942B	95.0	42.04	7.9	13.5	15[2]
71	February	15	A16SG	Calendered	97.6	34.3	16.2	5.24	19[3]

[1]Tested at Montana College of Mineral Science and Technology
[2]Tested at University of Utah
[3]Two layer laminates
[4]Heterogeneous grain size of 7 to 70 and some voids

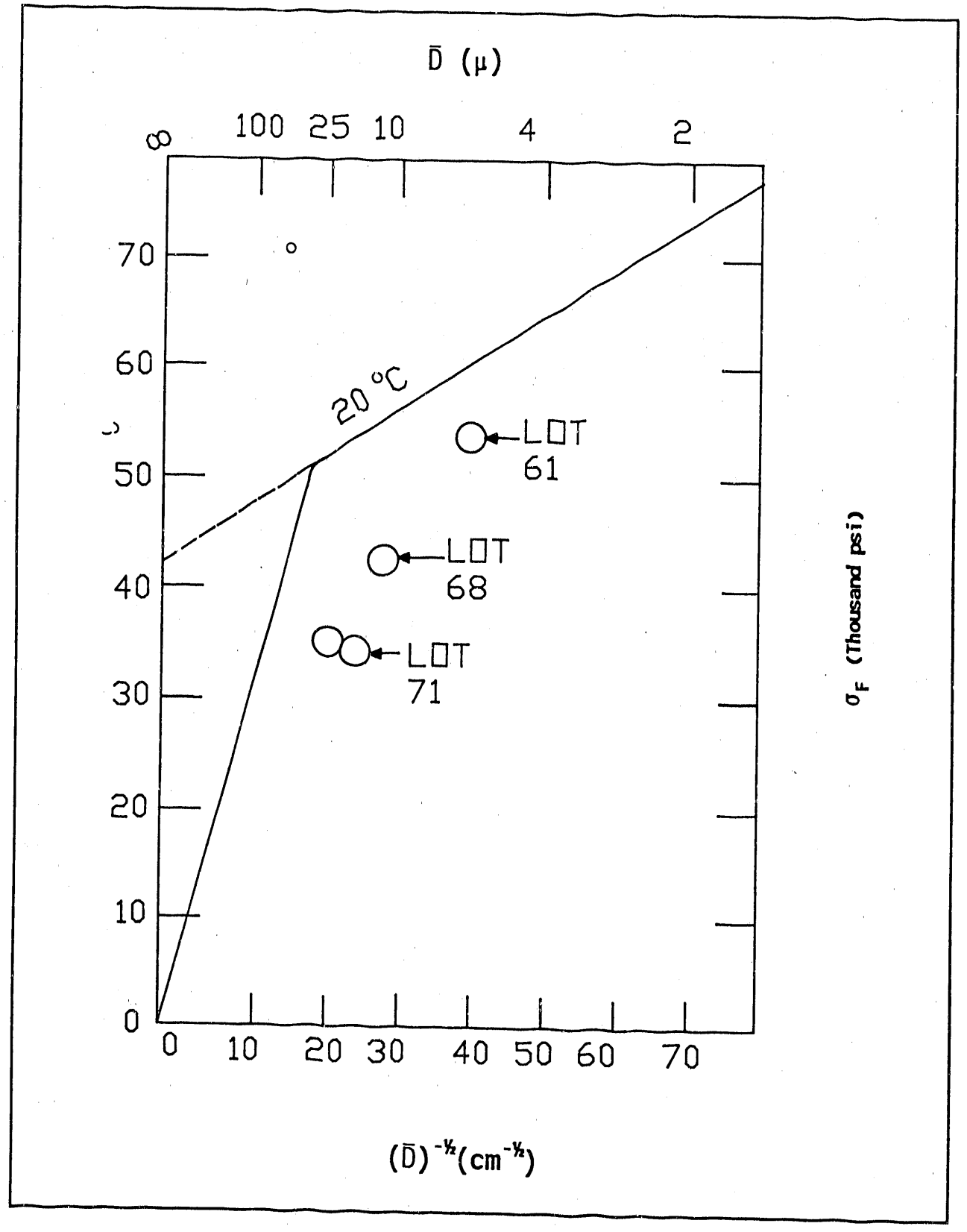

FIGURE 9 -- DEPENDENCE OF FLEXURE STRENGTH

The Knudsen equation implies completely elastic behavior in which large grains fracture by transgranular cleavage. Smaller grains deflect cracks at the grain boundaries and, therefore, fracture intergranularly along grain boundaries. The critical grain size for the transition from transgranular to intergranular fracture varies with the chemical composition and the temperature.

Deviation from the experimental curve of Figure 9 presented by Carniglia for alumina ceramics can be caused by the porosity since sintered densities of CCF ceramics vary from 95 to 97 percent theoretical compared to 98 percent for the data of Spriggs.[3] Another source of deviation is the grain-size distribution, which may be relatively tight or quite broad. Doping with MgO (0.03 percent) tends to refine grain size by inhibiting grain growth and avoiding formation of giant grains, which substantially reduce average strength.

Above 20 microns, grains tend toward elongated growth as compared to equiaxed grains below 15 μm. Porosity, grain-size distribution, and texture tend to modify the grain size versus strength relationship. Attaining higher strength requires high density (>98 percent theoretical) combined with fine, uniform grain size (<3 μm). This microstructure will allow 60- to 80-ksi (411 to 548 MPa) flexure strengths.

3.2.2.2 Subtask 2B-2 -- Short Rod Fracture Toughness Testing

No activity was scheduled or performed this quarter.

3.2.2.3 Subtask 2B-3 -- Fracture Testing of Joints

No activity was scheduled or performed this quarter.

3.2.2.4 Subtask 2B-4 -- Diametral Compression Test

No activity was scheduled or performed this quarter.

3.2.2.5 Subtask 2B-5 -- Microindentation Fracture Toughness Test

No activity was scheduled or performed this quarter.

3.2.3 Subtask 2C -- Development of Ceramic Specimens for Laminated Bond Testing

Laminated in-house bars were fabricated from lot 71 (A16SG powder) and made into strips, which were compacted by calendering to a thickness of 3 mm. The bilayer strips were partially browned to toughen the CCF material so they could be cut into 5-mm wide, 60-mm long strips. These bars were then fully debindered and sintered at 1,650 °C for 8 hours. The sintered bars showed no indication of a visible bond line at X 50 magnification.

The laminated bars were then broken on the four-point bend fixture. Average strength was 34.3 ksi (236.7 MPa) with a standard deviation (coefficient of variance) of 16.2 percent, giving a Weibull modulus of 5.24. The Weibull distribution of lot 71 is plotted in Figure 10.

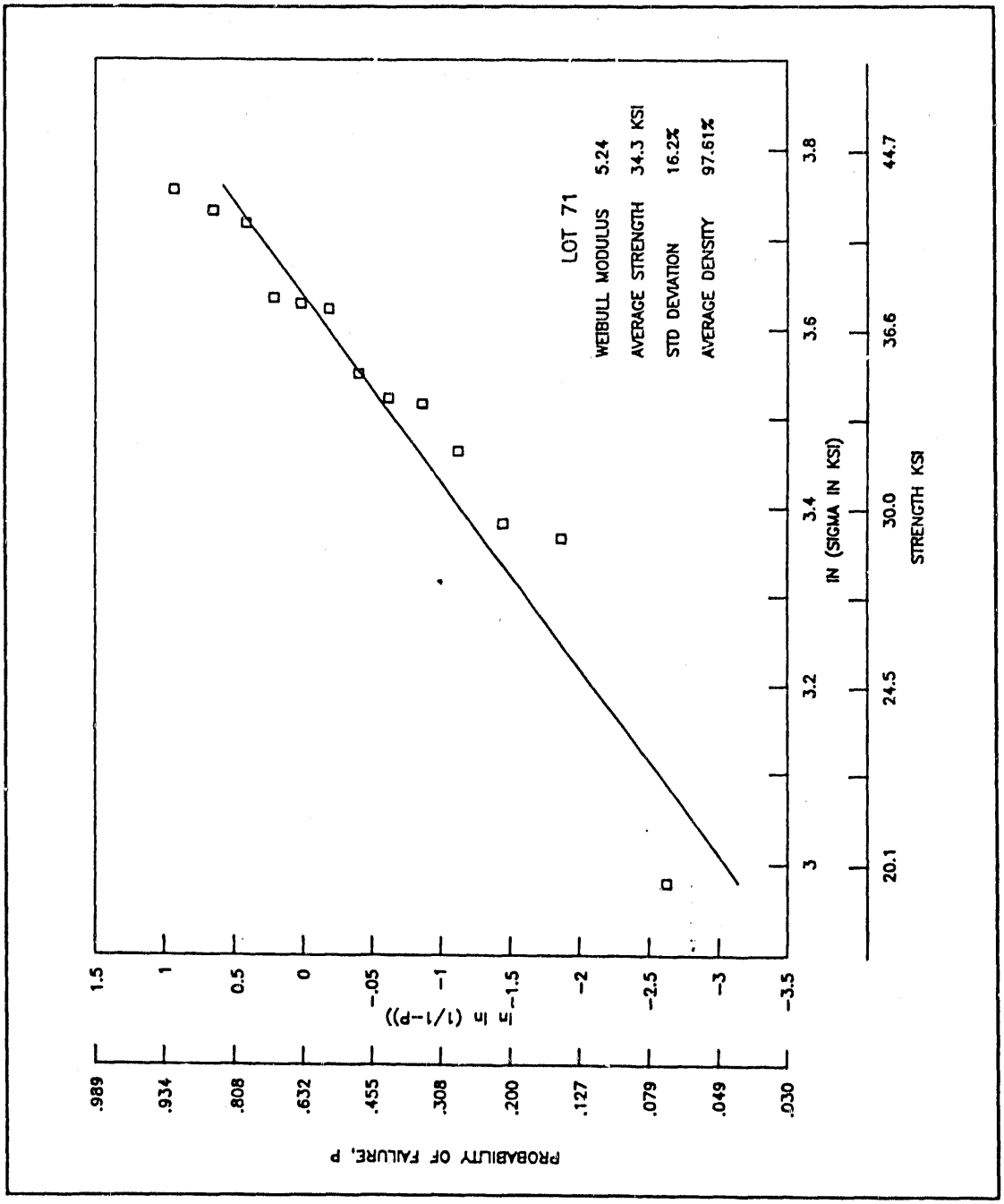

FIGURE 10 -- WEIBULL DISTRIBUTION FOR LAMINATED MOR BARS, LOT 71

The sintered density of the laminate slab was determined to be 97.6 percent. The bars were sectioned and examined with scanning electron microscopy to obtain a detailed microstructure of the joint. Even at X 2100, no lamination bond line was distinguishable. The microstructure (X 500) is shown in Figure 11 indicating an average grain size of 19 microns.

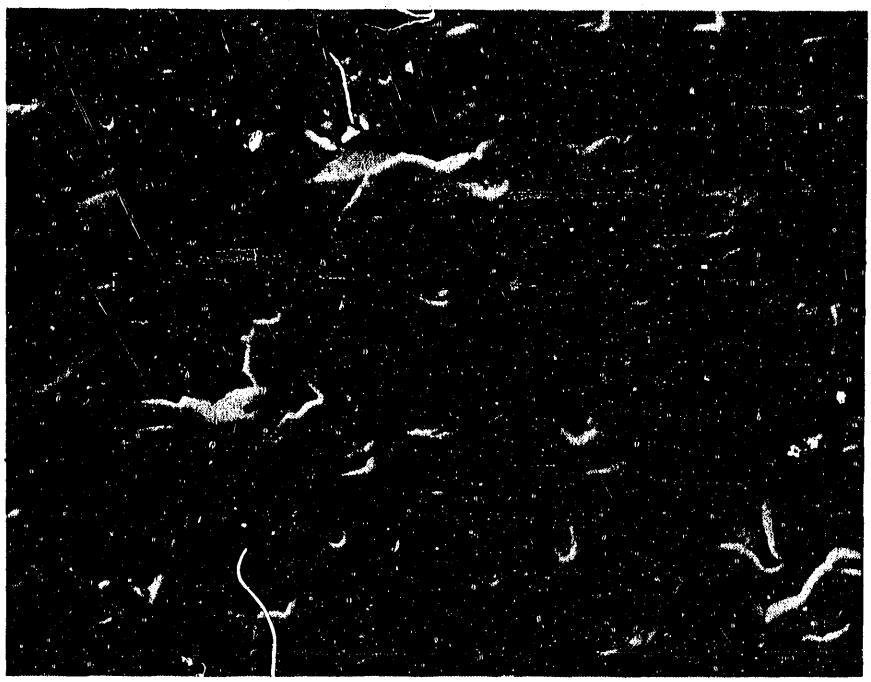

FIGURE 11 -- MICROSTRUCTURE OF LAMINATED SAMPLE, LOT 71

The relatively larger grains of lot 71, which were probably caused by the heat balance problem discussed in Section 3.2.1.1.3, resulted in lowered strength compared to lot 61 (see Table 3). Since the strength reduction can be explained by the larger grain size and since there was no evidence of bonding line fractures or porosity, the feasibility of lamination by the CCF process without producing strength degrading bonding flaws has been demonstrated.

Poor technique will produce gross lamination flaws. Over application of solvents (such as acetone) to the laminating surfaces will produce blisters. Overly dried surfaces will form weak, erratic, or unbonded layers resulting in delamination during the browning step. This delamination due to dry contact surfaces will occur even if strong compaction forces are applied to bond the laminate layers. ATL has obtained encouraging results by applying an acetone-thinned slurry of the alumina CCF organic mixture to both surfaces. Good bonds are obtained with relatively moderate compaction forces.

3.2.4 Subtask 2D -- Ceramic Matrix Composites Using the CCF Process

Fiber reinforced ceramic matrix composites are material systems of particular interest for high stress ceramic component applications under study in the Task 1 and Task 3 efforts of this program. During this quarter, ATL initiated an experimental program to study the initial aspects of fiber reinforced composites produced with the CCF process.

The standard CCF binder formulation incorporating A16SG alumina powder was selected for use as the green ceramic matrix for initial experiments. Dupont FP continuous alumina fiber was obtained and was used as a continuous oriented fiber reinforcement.

Polycrystalline ribbon fibers of alumina (approximately 5 by 25 microns in cross section and about 20 to 50 μm in length) were made at ATL using a cold spinning process (Section 3.2.1.1.1) on CCF/A16SG alumina.

Initial experiments with the Dupont FP continuous fibers in an oriented construction showed that fiber coating is probably necessary to eliminate cracking and delamination of the composite due to differential shrinkage between the green matrix and the fully fired fibers. Preliminary fiber coating experiments with organic coatings at hand did not appear promising. It is recognized that chemical vapor deposition (CVD) is frequently used for coating fibers for composite use. However, CVD is an expensive process step in most cases, and CVD capability is not set up at present in the laboratories. Further study of the continuous fiber coating problem is in progress.

ATLTM alumina fibers (fully fired at 1,650 °C) were incorporated into a small portion of standard green CCF mix by rolling the mix into a thin sheet, coating one surface with fibers, folding repeatedly and intermixing the fibers with the green ceramic matrix by extended processing on a compounding roll. The randomly oriented fibers constituted 12.4 volume percent of the binder-free composite. MOR bars were fabricated: five monolithic and five double layer laminated bars. These bars were then debindered and sintered according to current CCF procedures.

Densities of the fired bars were found to be low (86.7 percent theoretical for the monolithic bars, and 85.2 percent theoretical for the double layer laminated bars). Similarly, MOR values determined on the monolithic bars averaged 19.1 ksi compared to 11.1 ksi average for the laminated bars. The value for the monolithic material is less than one half of that customarily obtained for CCF monoliths of >95 percent theoretical density.

The surface finish seems to be an important controlling factor for strength. In fact, the green tape was cut into MOR bars using a knife. The surfaces of the bars were not smooth compared to the surface of the extruded bars or machined bars. The lower density is also responsible for the lower strength. Apparently, fiber loading works to limit sintering consolidation (a common situation with many fiber-containing ceramic bodies). The laminated, fiber reinforced bars displayed severe delamination on breaking, and only two samples were evaluated. Thus, it is not appropriate to attribute the very low MOR values only to low density, as the degree of bonding of the bars was clearly inferior. An improved bonding/laminating technique has been identified subsequent to this initial lamination experiment and appears to yield improved bonding. Further experiments with laminated, fiber-containing composites will use this new bonding technique.

3.3 TASK 3 -- CERAMIC FABRICATION AND MANUFACTURING

3.3.1 Subtask 3A -- Solid Oxide Fuel Cell

During the preceding quarter and the first several weeks of this quarter, the primary goal of Task 3 was to fabricate a stack of four individual cells. Although this was achieved, the overall integrity of the fuel cells was unacceptable. Consequently, the next goal was to develop a method of evaluating the individual cells to increase the overall integrity of the fuel cell stack. Relatively little effort was devoted to the latter goal since the overall effort of Task 3 was shifted to other programmatic goals during the first part of the quarter.

Since the initial overall goal during this quarter was to produce a stack of individual cells, CBSi personnel began to mass produce the individual cells, producing 12 to 30 individual cells per day. The primary goal was to produce cells that would be conducive to stacking; therefore, some of the internal cell features previously developed were eliminated to allow the production of more cells. Two different approaches were taken to develop the four-high fuel cells.

1) Individual cells were produced using the standard techniques developed in preceding months. These individual cells, which consisted of a separator plate and two membranes, were debindered, and the debindered cells were joined with the green CCF material to form a four-high stack. The cells were then debindered a second time.

2) In the second technique, the standard technique was also used, but the entire stack was pressed together in a Carver press while all the materials were in the green state.

The actual assembly of cells is highly dependent on the fill material used to support the material in the green and brown (debindered) state. The primary accomplishment was the refinement of the previously developed assembly details. Cell debindering was a significant problem, largely overcome by supporting the green fuel cell assembly on pads of Pellon material, which was then supported on metal screens. This allowed the binder to be removed equally from both the top and bottom (and in between) cells, which prevented exaggerated warping in the brown state. The flatness of the brown material continually improved.

The primary problems during development efforts were material warping in the final firing and the general lack of membrane bonding to the separator plate.

The warping during firing was expected because of the overall complexity of the part and the fact that the part has significant shrinkage during sintering (as do all ceramics). The techniques used during the browning stage to increase the flatness are being incorporated into the final firing stage; however, high temperature Pellon and screen equivalents have not been found.

The problems associated with the general decay of bonding in the samples was not expected. Since the overall improvement in the CCF process was occurring at the same time as the fabrication development, it was difficult to accurately pinpoint the exact cause of the bonding failure. It was pinpointed to the technique used to mass produce the cells. During mass production, paper was placed on the CCF material to prevent contamination of the laboratory environment. Later, it was found that the paper altered the binder at the surface of the material and caused the bonding problem.

3.3.2 Subtask 3B -- MHD Electrode Fabrication

MSE personnel completed the MHD electrode design during the first part of this quarter (Task 1). In general, the strict material requirements indicate that relatively few materials can be used in this fast startup MHD environment. One of the materials that appears promising is molybdenum disilicide ($MoSi_2$). Although pure $MoSi_2$ does not have the required thermal properties, these properties can be achieved by chemically grading the $MoSi_2$ with other materials to increase its resistance to thermal stress. Consequently, the near-term goal of Task 3 is to investigate the possibility of using the CCF process with $MoSi_2$. One advantage of the CCF process is the ability to produce graded ceramics.

During this quarter, work on the $MoSi_2$ electrode was initiated by obtaining commercial, high purity $MoSi_2$ powder. A preliminary sample was prepared with the CCF binder, and the sample was debindered using the standard procedures used for alumina. The material browned (debindered) without powder oxidation. This is

important, since there was some concern that the pure $MoSi_2$ powder would readily oxidize at the temperatures used in the browning cycles. However, the samples did not sinter when fired at 1,600 °C for 2 hours (the standard cycle used for alumina).

Relatively little literature exists on the pressureless sintering of $MoSi_2$--most of this literature concentrates on hot pressing $MoSi_2$ in reducing environments. Consequently, the first task undertaken was to identify potential sintering aids that could be used to increase the density of $MoSi_2$. Silicon carbide (SiC) sintering aid literature was reviewed to see if sintering aids used in SiC could be used in $MoSi_2$. Since commercial $MoSi_2$ produced by Kanthal has up to 20 volume percent glass phase mixed with the $MoSi_2$, fused silica was added to the $MoSi_2$ to see if fused silica would act as a sintering aid.

Initial attempts to sinter $MoSi_2$ mixed with silica were unsuccessful when fired in air; therefore, work was conducted sintering $MoSi_2$ in an argon atmosphere. Firing the samples in argon was suggested by personnel at Los Alamos National Laboratory, who noted that $MoSi_2$ fired to good densities in argon between 1,750 to 1,850 °C but would not densify in the presence of oxygen.

An Astro furnace was rebuilt to fire the $MoSi_2$ in argon at approximately 1,800 °C. The first samples fired, disks pressed with the CCF material, resulted in reasonably competent pieces. Since the materials were fired on graphite, the $MoSi_2$ reacted with the graphite and formed SiC. During later firings, the $MoSi_2$ was placed on SiC grit so the green SiC surface layer would not form.

Powder x-ray diffraction traces were run on samples of the pressed $MoSi_2$ fired in the Astro furnace. The most prominent phase identified was $MoSi_2$ and some secondary phases were tentatively identified: SiC and Mo_5Si_3. Comparing these samples to other $MoSi_2$ samples made using the normal CCF material, the amount of the secondary phases increases with increasing binder content. This change of phases is graphically demonstrated in Figure 12. The top graphic in this figure is the x-ray diffraction pattern of commercial $MoSi_2$; this pattern indicates the commercial material is basically pure $MoSi_2$ (the glass phase will not appear on x-ray diffraction patterns).

It appears that a consequence of excess organic binders mixed with $MoSi_2$ is the formation of SiC and Mo_5Si_3. A possible reaction is:

$$5MoSi_2 + 7C == 7SiC + Mo_5Si_3$$

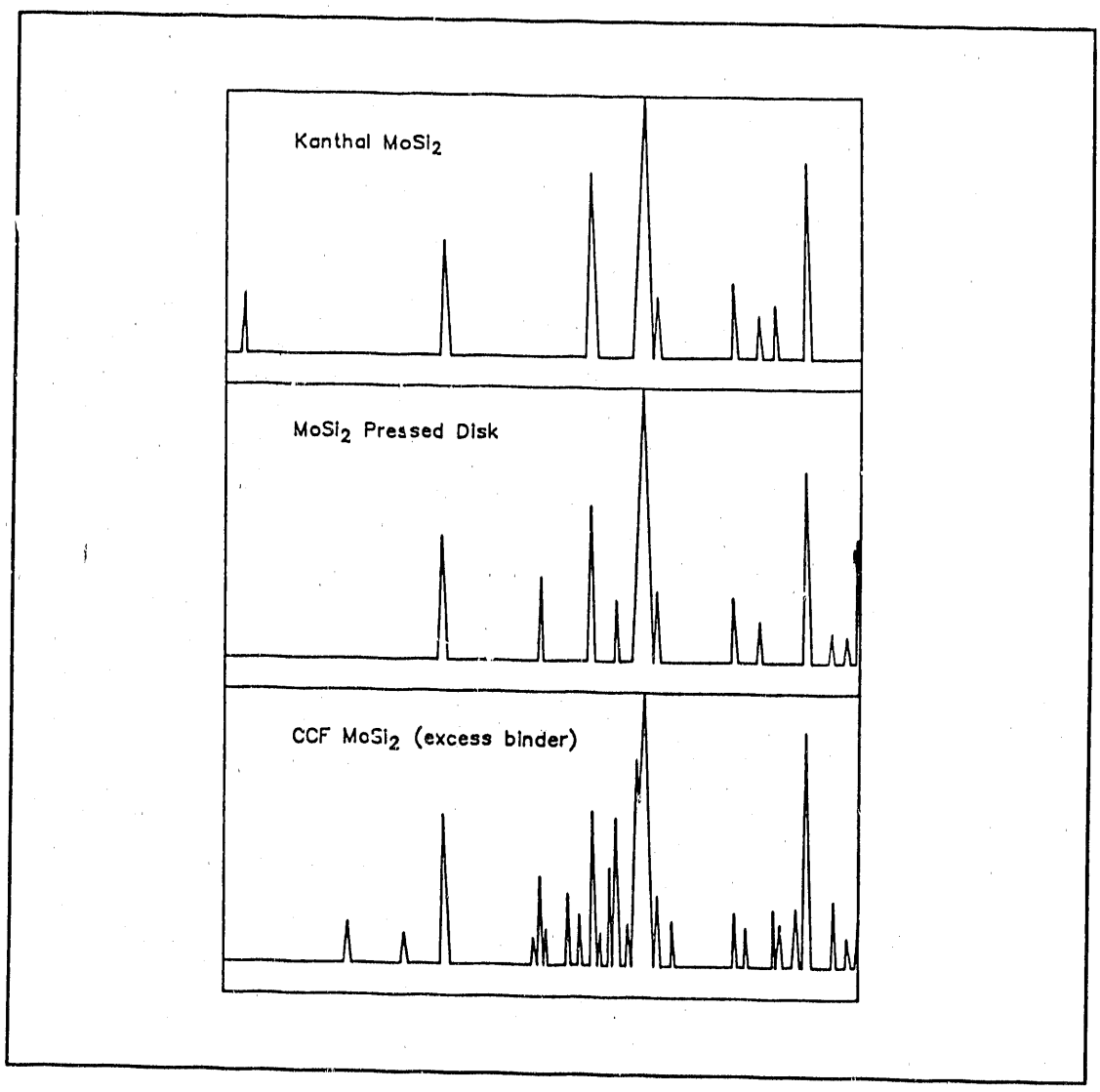

FIGURE 12 -- COMPUTER RECREATED X-RAY DIFFRACTION DATA

Three dopants have been used successfully to densify $MoSi_2$, dry pressed pellets, TiO_2, MnO_2, and B_2O_3. A 0.6 weight percent dopant concentration in $MoSi_2$ pellets having 14.4 weight percent silica allows sufficient densification at 1,800 °C with a 2-hour hold time, for self-supporting oxidation resistance when exposed to air at 1,400 °C. One limiting factor in achieving greater densities appears to be an excessive weight loss during sintering, up to 20 weight percent more than expected.

Sintered pellets were tested for oxidation resistance as follows; pellets were heated in air at 200 °C/hr to 1,400 °C and held for 2 hours. Each of the three 14.4 weight percent silica/doped pellets produced an outer glass coating during the oxidation test. Samples not containing dopants or samples containing less than 14.4 weight percent silica oxidized to a powder during the 1,400 °C test.

All sample pellets sintered in the Astro furnace were electrically conductive. After the 1,400 °C oxidation test, the doped samples all had a high electrical resistance when measured on the sample exterior but had a low resistance once the glass was removed.

As a possible alternative to the silica doped samples, zircon doped $MoSi_2$ samples were formulated. Several possible advantages for doping with zircon instead of silica may exist, assuming zircon will form a protective layer for the $MoSi_2$. These possible advantages include: increased maximum operation temperature, increased creep resistance, and toughening. Samples containing 10 weight percent zircon, without sintering aids, achieved adequate density to withstand the 1,400 °C oxidation test; however, these samples did not have an apparent silica glass coating on the surface. The three previous mentioned sintering aids, B_2O_3, TiO_2, and MnO_2, did not improve the oxidation resistance of $MoSi_2$, having 19.4 weight percent zircon. Samples containing 19.4 weight percent zircon, both doped and undoped, exhibited almost a two-fold volume increase during the oxidation test, and the samples had a weight loss of nearly 30 weight percent.

3.3.3 Subtask 3C -- High Stress Component Fabrication

Task 3 will concentrate on developing a high stress, alumina armor component reinforced with a variety of additives. During the first part of this quarter, preliminary work on additive additions for alumina was done. Silicon carbide (SiC) additions were investigated at the end of the quarter.

The two primary goals of the SiC/alumina system investigation are to determine the alumina system used to form the SiC composite and, second, to establish a data base that can be used to establish the impact of adding SiC whiskers to alumina using the CCF process.

The primary problem associated with adding SiC whiskers to alumina is that whiskers impede the densification. This problem is unrelated to the CCF process but arises using other systems that require sintering to achieve densification. If the sintering temperature is increased to achieve greater density, the SiC whiskers degrade or react with alumina. The usual solution to this problem is to hot press or hot isostatically press the alumina material. Unfortunately, this is an expensive process and is not applicable to mass production of economical parts.

Another technique others have used is to add sintering aids to the alumina, thereby, reducing the sintering temperature. The primary sintering aid technique is to add liquid phase sintering aids. Using this technique, 15 volume percent of SiC whiskers may be added, and reasonable densities can be achieved (greater than 85 percent theoretical) by firing at a high temperature in argon. Another technique is to use a more reactive alumina, one that sinters around 1,200 °C so the material will still sinter with the addition of SiC whiskers at an increased temperature.

The first approach will leave a glassy phase in the grain boundaries and may lower the impact resistance of the alumina for armor applications. The second method is more difficult to achieve, since the process used to increase the alumina's activity is not yet commercially developed.

During this quarter, personnel explored the use of other sintering aids to lower the sintering temperature of alumina. The three aids selected were TiO_2, Fe_3O_4, and MnO_2. These three aids, according to the literature, increase the number of vacancies in the alumina, which increases the oxygen mobility and consequently the sintering rate. Ideally, these compositions will not form a liquid phase nor will the aids concentrate in the grain boundaries.

Seven different compositions of alumina mixed with different sintering aids were evaluated. In all cases, 2 weight percent of the aids was added to the alumina. Three of the compositions were the pure aid mixed with the alumina, three more of the compositions had uniform mixtures of two aids (50 percent each), and the final composition had a uniform mixture (33 percent each) of the three aids. The mixture compositions are shown in Figure 13.

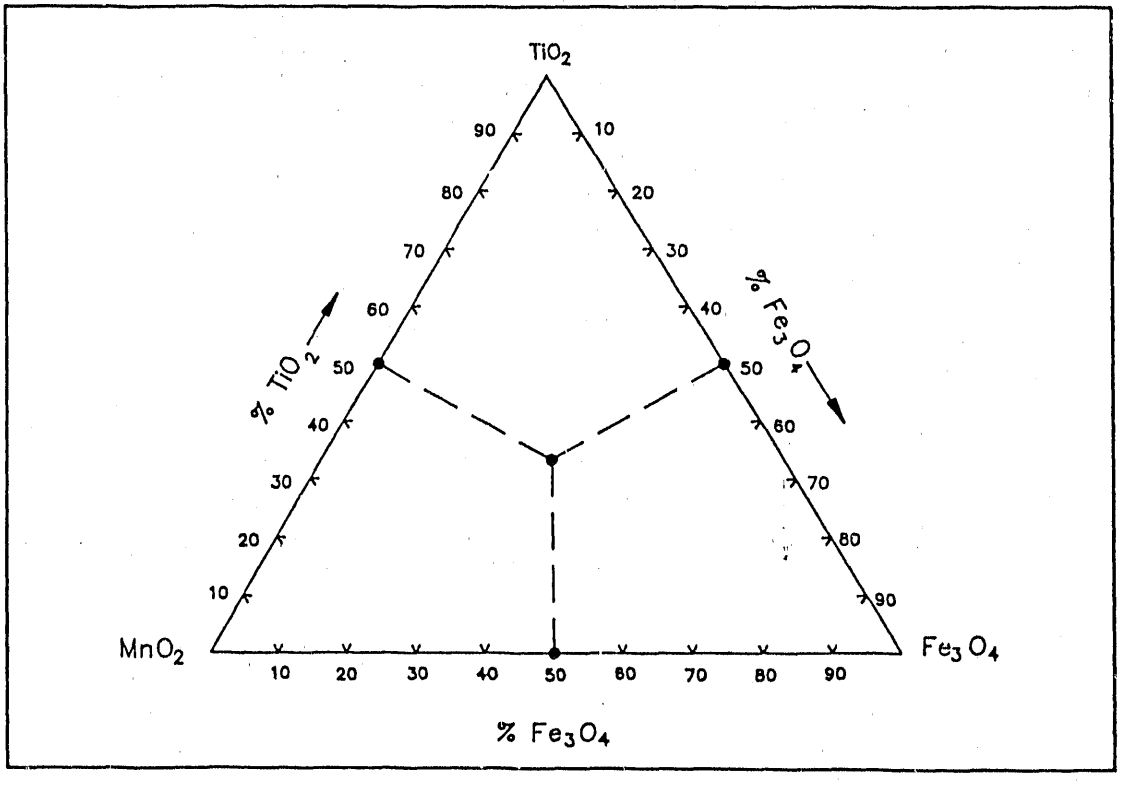

FIGURE 13 -- MAP OF THE DOPANTS USED TO LOWER THE SINTERING TEMPERATURE

Three criteria were used to evaluate the effect of the sintering aids: density, microstructure, and hardness. All of the samples were fired at 1,200, 1,250, 1,300, 1,350 and 1,640 °C. All samples were held at the firing temperature for 2 hours. The samples were evaluated after firing. Density measurements were taken on all samples, while the microstructure and hardness measurements were taken on samples fired to 1,300 °C.

These property measurements are graphically shown on ternary plots. The property measurements are overlaid on the diagram where the chemical composition would occur on that diagram. These diagrams, Figures 14 through 17, show the density of the seven compositions at both 1,200 and 1,300 °C; the hardness of 1,300 °C samples; and an indication of the microstructure of the seven samples.

Since the goal of the dopant studies is to achieve density at the lowest possible temperature without compromising the ceramic materials; three of the dopant combinations may be excluded after viewing Figures 14 and 15. The densities of the lower part of the diagram are not adequate. Therefore, the pure MnO_2, the MnO_2-Fe_3O_4, and the pure Fe_3O_4 materials are discarded based on density considerations.

In Figure 17, the microstructure of the TiO_2-Fe_3O_4 sample is decidedly inferior to the three remaining materials, since 10 percent of the total grains have an exaggerated grain growth. Long grains, with a 3 to 4 aspect ratio and straight sides, are considered exaggerated. Exaggerated grain growth often indicates the presence of a liquid phase during sintering. If this liquid phase stays at the grain boundaries, the mechanical properties of the ceramic will be compromised.

The best microstructure is the TiO_2 doped material, since it has the smallest grain size and none of the grains are exaggerated. Likewise, the next best microstructure is that of the tridoped material, which also has no exaggerated grains but a sightly larger uniform grain size of 10 microns.

Figure 16 shows the diamond pyramid hardness of the alumina material. It can be seen that the tridoped material and the TiO_2-MnO_2 material have the best hardness. Since the goal of the current program is to choose a dopant chemistry that functions well, but is not necessarily optimized, the tridoped material was selected as the material for further study. The final selection is based on the slightly better microstructure of the tridoped material compared to the TiO_2-MnO_2 system, which has similar properties.

Toward the end of quarter, CBSi obtained an alumina powder (most likely Reynolds RC-HP alumina) containing 20 weight percent Tateho SiC whiskers. The main objective of the experiments was to determine if near theoretical densification of the body occurs during sintering. Concerns include the ability to remove the residual carbon during sintering, the extent of shrinkage resistance created by the whiskers, and whether the SiC whiskers are inert and retain their physical properties.

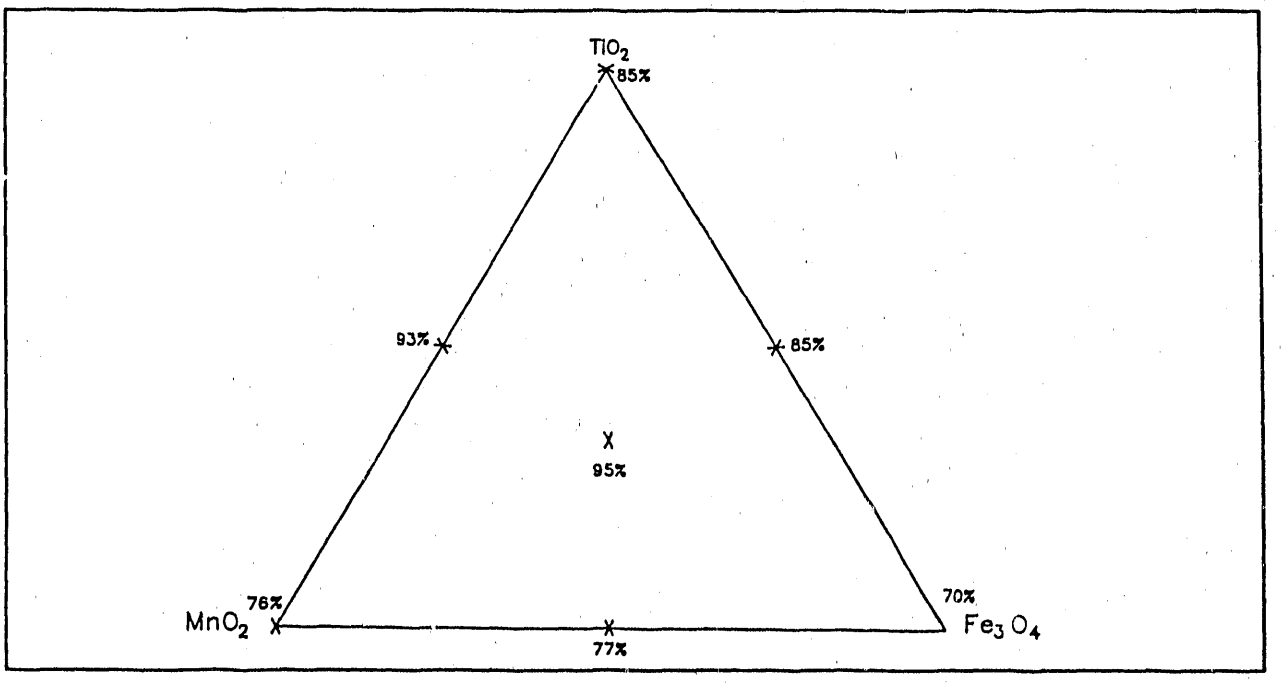

FIGURE 14 -- DENSITIES OF THE SEVEN SAMPLES FIRED AT 1,200 °C

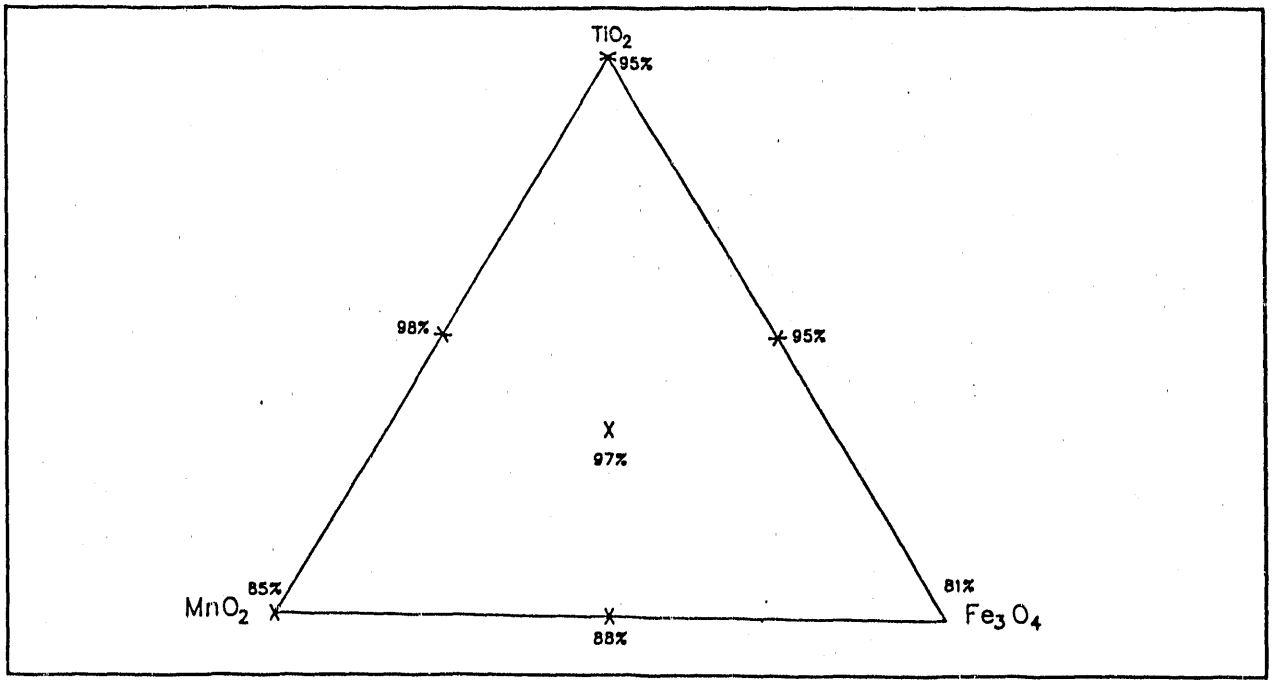

FIGURE 15 -- DENSITIES OF THE SEVEN SAMPLES FIRED AT 1,300 °C

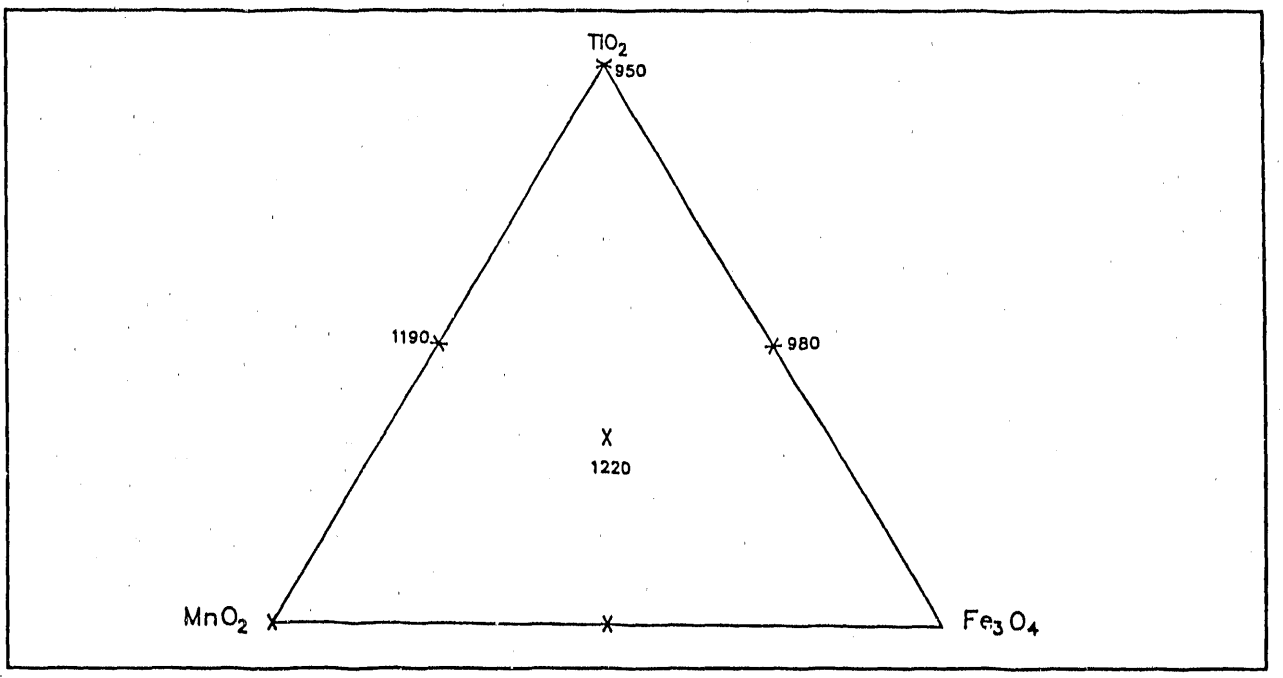

FIGURE 16 -- HARDNESS OF THE FOUR SAMPLES WITH THE BEST DENSITIES AT 1,300 °C

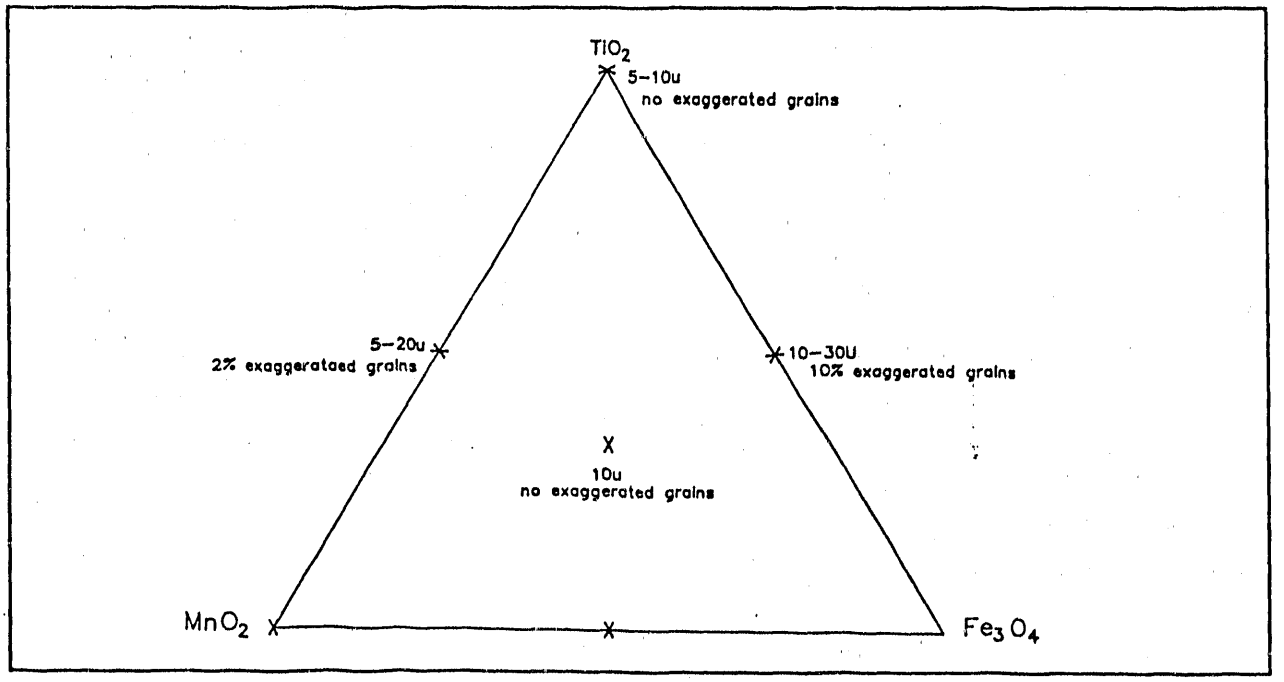

FIGURE 17 -- MICROSTRUCTURE OF THE DOPED ALUMINA SAMPLES

A graphite heating element furnace (4.5-in. diameter Astro furnace) was used to fire the samples. Since the alumina powder is already blended with 20 weight percent SiC whiskers, dopants and diluting amounts of uncompounded alumina were added to complete the sample series. Table 4 shows the density results for samples without sintering aids and with 1 weight percent tridope (⅓ Fe_2O_3, ⅓ TiO_2, ⅓ MnO_2) added. From the results, sintering the whisker-containing samples was not adequate; only 60 percent of the theoretical density was achieved for the 10 weight percent whisker samples, doped or undoped.

TABLE 4 -- CHARACTERIZATION OF SiC WHISKER REINFORCED ALUMINA PRESSED PELLET SAMPLES

CERAMIC	WEIGHT PERCENT SiC WHISKERS		
	0	10	20
Alumina			
Density (percent theoretical)	94.0	60.0	--
Diametric Shrinkage (percent)	16.9	7.0	3.0
Thickness Shrinkage (percent)	16.12	15.4	4.8
Weight Loss (percent)	4.47	15.0	22.3
Tridoped (1 percent) Alumina			
Density (percent theoretical)	--	58.0	--
Diametric Shrinkage (percent)	6.4	--	--
Thickness Shrinkage (percent)	9.6	--	--
Weight Loss (percent)	15.4	--	--

Furthermore, weight loss in excess of the expected 5 weight percent was observed. Figure 18 shows a plot of shrinkage and weight loss for the undoped samples. X-ray data indicates the SiC whiskers disappear during sintering. The diffraction trace for this sample shows primarily alpha alumina with only two unidentified peaks. These peaks do not appear to correspond to possible phases listed in the powder diffraction file for SiC and aluminosilicates.

4.0 PLANNED ACTIVITIES

4.1 TASK 1 -- CERAMIC COMPONENT DESIGN AND ANALYSIS

4.1.1 Subtask 1A -- MHD Electrode Design and Analysis

This task is approximately 95 percent complete, and the remaining work is refining the design based on experiments to be completed by CBSi. It is necessary to establish the achievable densities in pure and graded $MoSi_2$. Some strength information will also be generated by ATL, and it will be used for the final design refinements. These results are expected to be generated during the next quarter, with the design being finalized in the subsequent quarter.

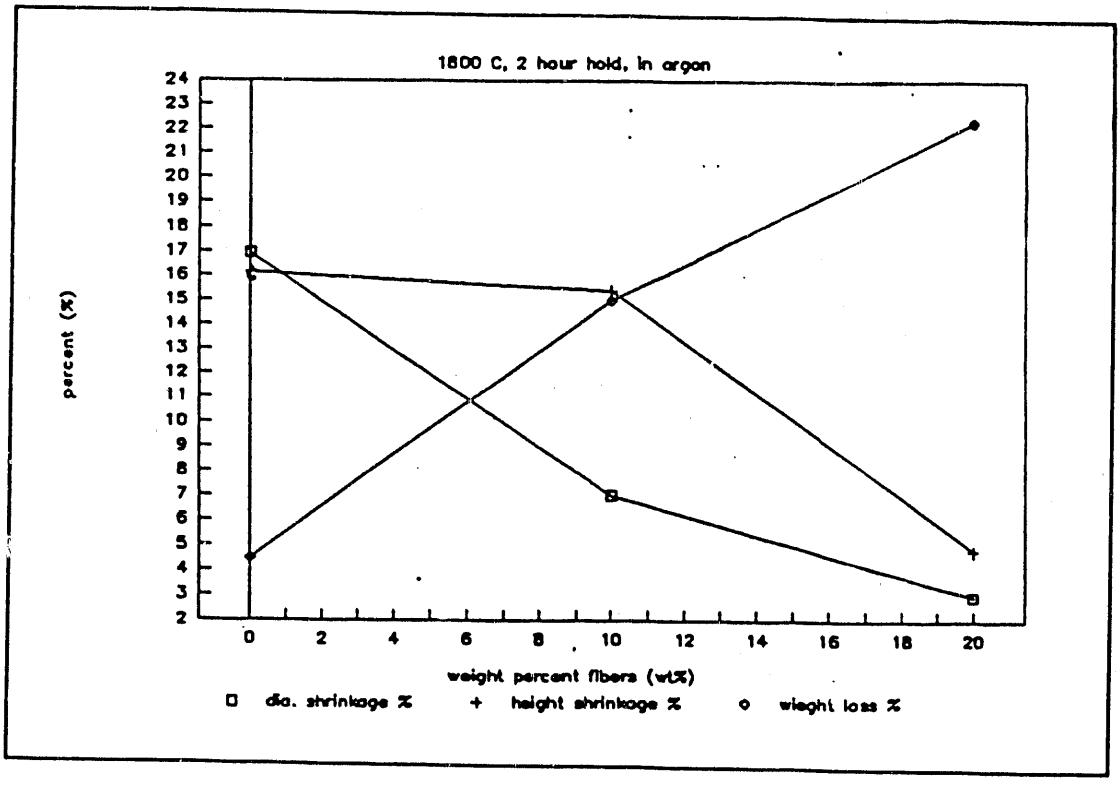

FIGURE 18 -- Al_2O_3 COMPACTS CONTAINING SiC WHISKERS

4.1.2 Subtask 1B -- High Stress Component Design and Analysis

With the recent decision to emphasize low cost fabrication and the subsequent change from whisker reinforcement to particulate reinforcement, modeling and analysis activity is not expected in this subtask during the next quarter.

4.2 TASK 2 -- EXPLORATORY DEVELOPMENT USING THE CCF PROCESS

4.2.1 Subtask 2A -- Characterization of Starting Materials

4.2.1.1 Subtask 2A-1 -- Ceramic Process Control Studies

Ceramic process control studies will be completed, and process optimization procedures will be tested and implemented wherever practicable. Lightweight plates made from CCF fibers will be fabricated and employed to minimize the furnace heat balance problem discussed in Section 3.2.1.1.3.

An optimum (or more optimum) temperature-time profile for the furnace based on the lower mass CCF fiber plates will be established. The optimization criteria are maximum sintered density and minimum grain size (preferably 1 to 3 microns). This improved profile should provide higher flexure strengths for the CCF processed alumina ceramic.

Debindering (browning) schedules will be studied to improve the machining characteristics (sawing, drilling, and turning) since each operation seems to require a different degree of curing.

4.2.2 Subtask 2B -- Mechanical Test Methods

4.2.2.1 Subtask 2B-1 -- Flexural Testing to MIL-STD-1942

Results of the 1,000 °C MOR bar tests at the University of Utah will be obtained and analyzed. Further testing of monolithic CCF process specimens will be performed as required to evaluate process control measures. Decisions will be made on whether to use in-house bars, MIL-STD-1942B bars, or both for process control experiment evaluations.

4.2.2.2 Subtask 2B-2 -- Short Rod Fracture Toughness Testing

Samples will be fabricated for preliminary short rod fracture toughness specimens. Some testing will be initiated during the next quarter.

4.2.2.3 Subtask 2B-3 -- Fracture Testing of Joints

Samples will be fabricated for joint fracture evaluation and preliminary testing will be initiated in the next quarter.

4.2.2.4 Subtask 2B-4 -- Diametral Compression Test

Some samples will be fabricated for diametral compression testing in the next quarter.

4.2.3 Subtask 2C -- Development of Ceramic Specimens for Laminated Testing

Laminated MOR test bars will be fabricated and tested in both the width-height and length-height orientations. Results will be compared with monolithic and width-length alignments during the next quarter.

4.2.4 Subtask 2D -- Ceramic Matrix Composites Using the CCF Process

Because economical SiC whiskers are unlikely, efforts will now be concentrated on particulate SiC reinforcement. CBSi is currently working on the composition to be selected; and when this is accomplished, ATL will begin generating density, flexure strength, microstructure, and related data.

4.3 TASK 3 -- CERAMIC FABRICATION AND MANUFACTURING

4.3.1 Subtask 3A -- Solid Oxide Fuel Cell

No work is planned on this project during the next quarter.

4.3.2 Subtask 3B -- MHD Electrode Fabrication

The project goal, as defined at the end of this quarter, is to produce a $MoSi_2$ structure with a seven layer, chemically graded structure. Each layer is 1- to 2-mm thick with a chemical composition ranging from 85 to 100 percent $MoSi_2$; the balance is silica or doped silica. The top and bottom layers are pure $MoSi_2$; the second and sixth layers contain 5 volume percent silica; the third and fifth layers 10 volume percent silica; and the final (center) layer has 85 percent $MoSi_2$ with 15 volume percent silica.

The emphasis next quarter will be to choose a standard $MoSi_2$/silica/dopant/binder composition and begin fabricating 1- to 2-mm thick layers using the tape caster, modified screen printer, and forming rolls. These sheets will then be pressed together, browned, and fired. Characterization will include density, microstructure, and phase analysis.

4.3.3 Subtask 3C -- High Stress Component Fabrication

The three primary goals of this task are: 1) finish characterizing the alumina powder mixed with SiC whiskers; 2) develop the requisite fabrication technology to manufacture large ceramic pieces (at least 4 inches by 4 inches by ½ inch to 6 inches by 6 inches by 1 inch); and 3) investigate particulate SiC additions to alumina because of potential for lower cost fabrication. Other alternatives may be possible.

5.0 TECHNICAL SUMMARY

5.1 TASK 1 -- CERAMIC COMPONENT DESIGN AND ANALYSIS

In Subtask 1A, a model electrode to be fabricated from layers of $MoSi_2$ graded with quartz glass additions up to 15 percent has been designed. This will demonstrate the applicability of the CCF process to a nonoxide material and also the ability of the process to readily fabricate graded structures. The electrode, designed around parameters reported in the preceding quarterly report, has been modeled and, through finite element analysis, has been shown to be capable of withstanding the steady-state and transient thermal stresses associated with generator operation. Joule heating was calculated and shown to be negligible compared to the heat flux of combustion origin.

Subtask 1B called for a high stress component design. A ceramic armor application was chosen based on the Al_2O_3-SiC system. This component will be modeled once the final composition, its structure, and approximate mechanical properties are determined.

5.2 TASK 2 -- EXPLORATORY DEVELOPMENT USING THE CCF PROCESS

Some satisfactory flexure strength data (MIL-STD-1942) has been obtained at room temperature. High temperature (1,000 °C) data is being obtained from an outside vendor. The CCF process is being reexamined using a set of matrix experiments to determine the most important variables involved with producing satisfactory specimens. The bonded region in a laminated sample was examined using scanning electron microscopy, and the indistinguishability of the bond line was verified.

5.3 TASK 3 -- CERAMIC FABRICATION AND MANUFACTURING

5.3.1 Subtask 3A -- Solid Oxide Fuel Cell

This effort was terminated early in the quarter after it became apparent that considerable work would be needed to solve the shape control and integrity problems encountered when integration of electrode stacks was attempted.

5.3.2 Subtask 3B -- MHD Electrode Fabrication

Initial work on the $MoSi_2$ electrode fabrication, a nonoxide application of the CCF process, was reasonably successful but showed the need for further work. This is proceeding.

5.3.3 Subtask 3C -- High Stress Component Fabrication

This task has been determined to be of the greatest importance, and effort will be concentrated on it. Initially, SiC whiskers were employed as a reinforcement to alumina, but since low cost fabrication was the goal, whisker incorporation will not be pursued. Since pressureless sintering is employed, development of sintering aids was seen as the first step. This has been successful, resulting in selection of the triple dopant TiO_2-Fe_3O_4-MnO_2.

6.0 REFERENCES

1. Petch, N. J., Progress in Metal Physics, 5, 1-52, 1954.

2. Carniglia, S. C., "Petch Relation in Single-Phase Oxide Ceramics," Journal of American Ceramics Society, 48, (11), 580-583, 1965.

3. Spriggs, R. M., Mitchell, J. B., and Vasilos, T., "Mechanical Properties of Pure, Dense, Aluminum Oxide as a Function of Temperature and Grain Size," Journal of American Ceramics Society, 47, (7), 323-327, 1964.

APPENDIX A -- Project Schedule

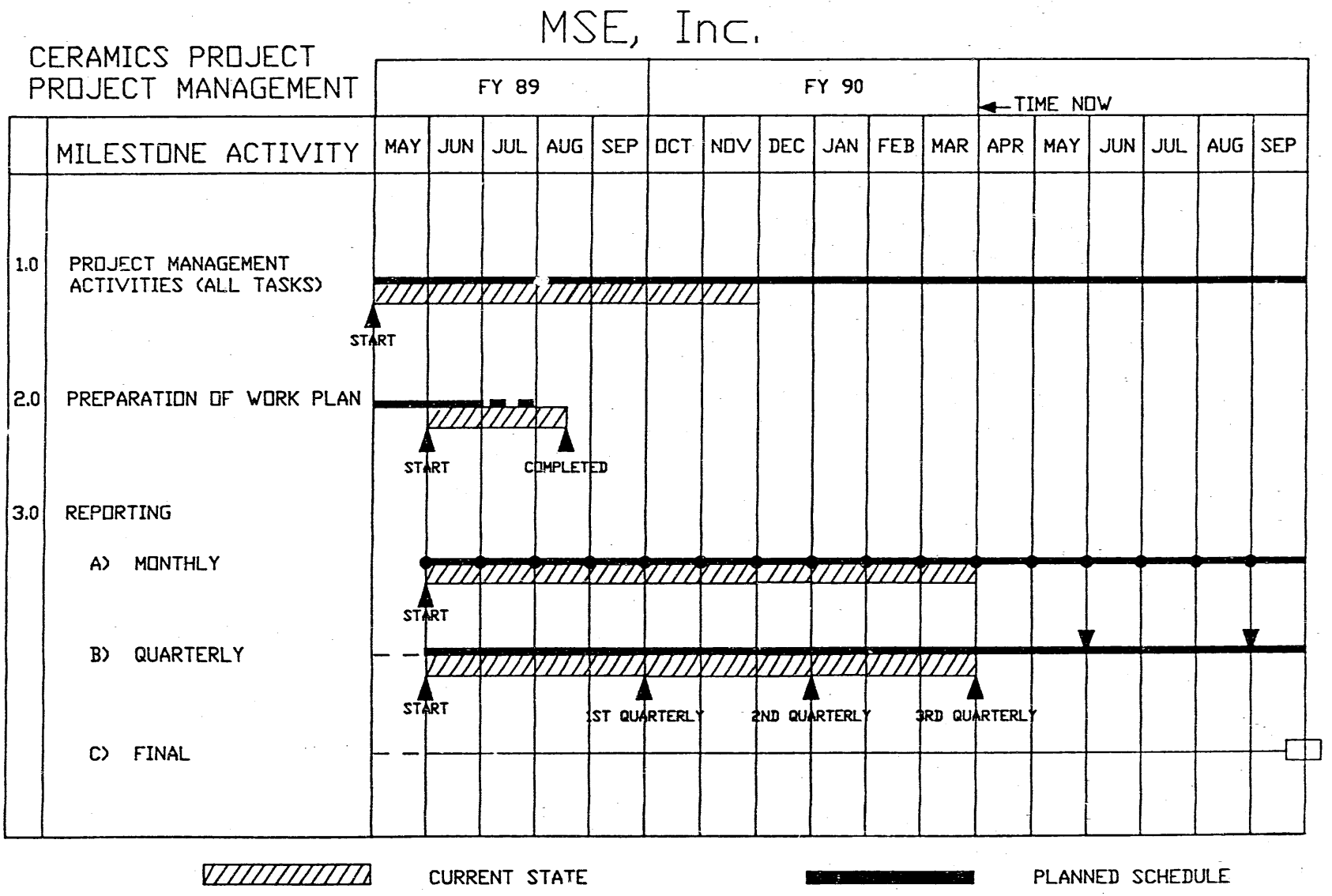
MSE, Inc.
CERAMICS PROJECT
PROJECT MANAGEMENT
FY 89
FY 90
TIME NOW
MILESTONE ACTIVITY
MAY JUN JUL AUG SEP OCT NOV DEC JAN FEB MAR APR MAY JUN JUL AUG SEP
1.0 PROJECT MANAGEMENT ACTIVITIES (ALL TASKS)
START
2.0 PREPARATION OF WORK PLAN
START
COMPLETED
3.0 REPORTING
A) MONTHLY
START
B) QUARTERLY
START
1ST QUARTERLY
2ND QUARTERLY
3RD QUARTERLY
C) FINAL
CURRENT STATE
PLANNED SCHEDULE

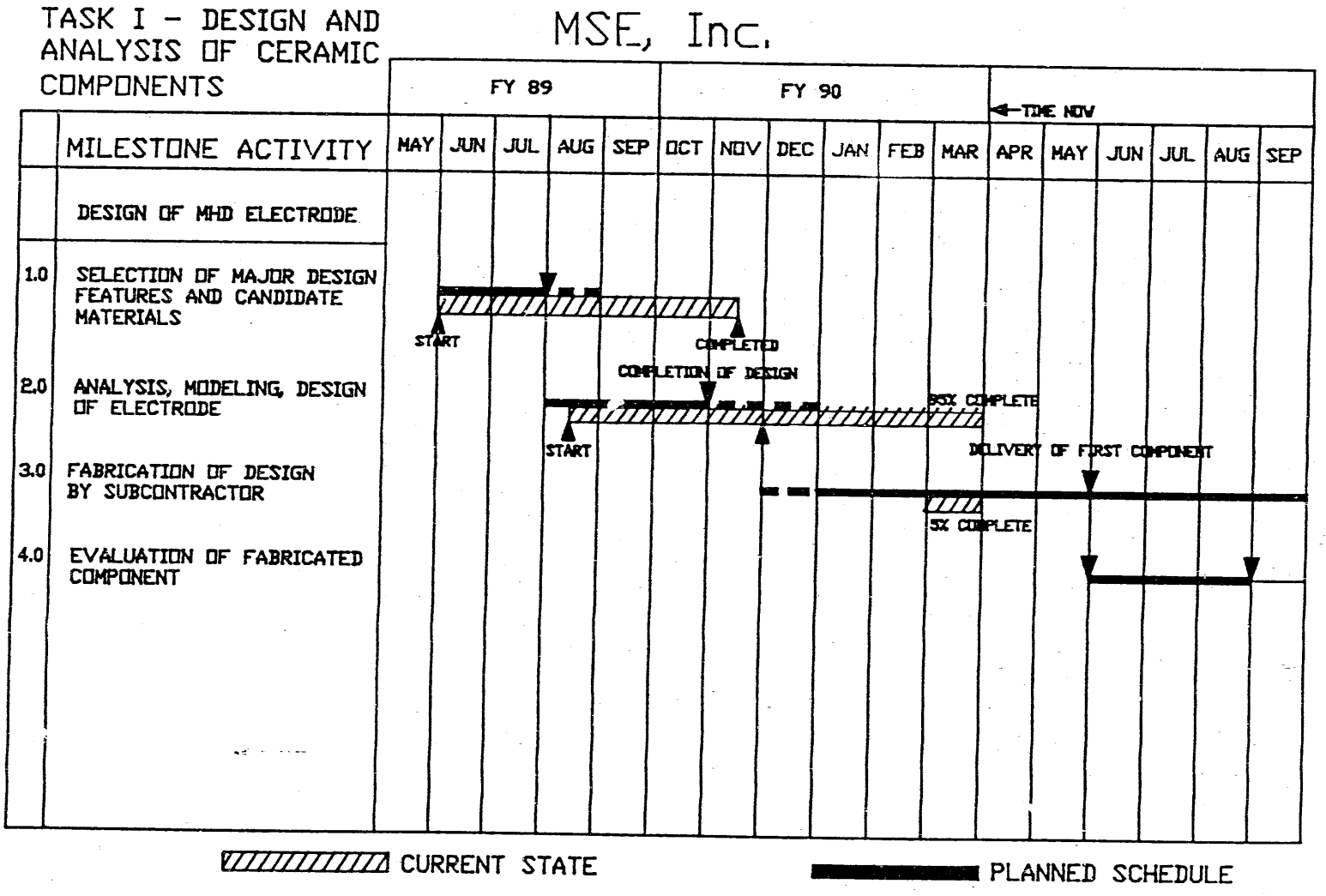
TASK I - DESIGN AND ANALYSIS OF CERAMIC COMPONENTS
MSE, Inc.
FY 89
FY 90
TIME NOW
MILESTONE ACTIVITY
MAY JUN JUL AUG SEP OCT NOV DEC JAN FEB MAR APR MAY JUN JUL AUG SEP
DESIGN OF MHD ELECTRODE
1.0 SELECTION OF MAJOR DESIGN FEATURES AND CANDIDATE MATERIALS
START
COMPLETED
2.0 ANALYSIS, MODELING, DESIGN OF ELECTRODE
COMPLETION OF DESIGN
85% COMPLETE
START
3.0 FABRICATION OF DESIGN BY SUBCONTRACTOR
DELIVERY OF FIRST COMPONENT
5% COMPLETE
4.0 EVALUATION OF FABRICATED COMPONENT
CURRENT STATE
PLANNED SCHEDULE

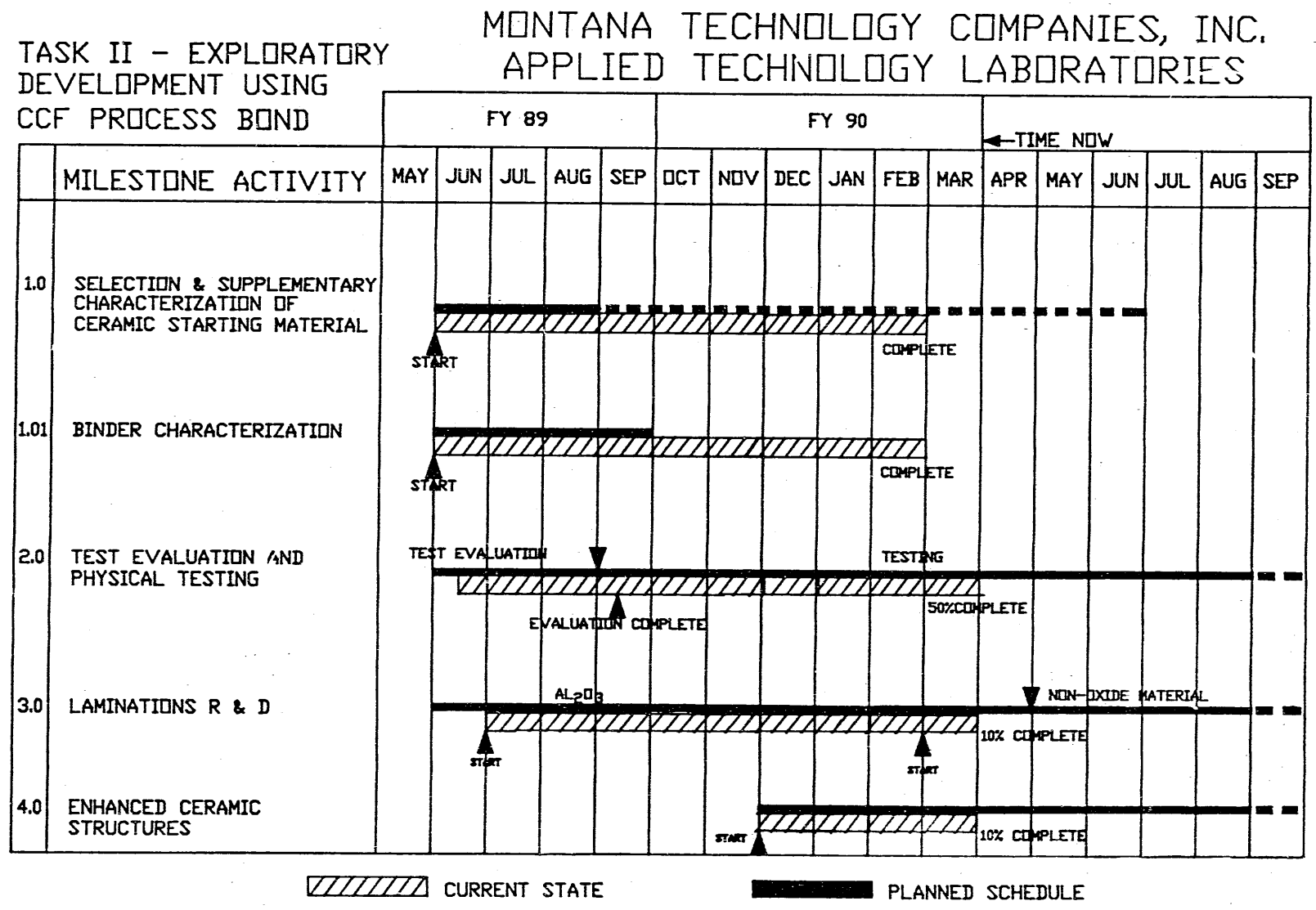
MONTANA TECHNOLOGY COMPANIES, INC.
APPLIED TECHNOLOGY LABORATORIES
TASK II - EXPLORATORY DEVELOPMENT USING CCF PROCESS BOND
FY 89
FY 90
TIME NOW
MILESTONE ACTIVITY
MAY JUN JUL AUG SEP OCT NOV DEC JAN FEB MAR APR MAY JUN JUL AUG SEP
1.0 SELECTION & SUPPLEMENTARY CHARACTERIZATION OF CERAMIC STARTING MATERIAL
START
COMPLETE
1.01 BINDER CHARACTERIZATION
START
COMPLETE
2.0 TEST EVALUATION AND PHYSICAL TESTING
TEST EVALUATION
TESTING
EVALUATION COMPLETE
50%COMPLETE
3.0 LAMINATIONS R & D
Al_2O_3
NON-OXIDE MATERIAL
START
START
10% COMPLETE
4.0 ENHANCED CERAMIC STRUCTURES
START
10% COMPLETE
CURRENT STATE
PLANNED SCHEDULE

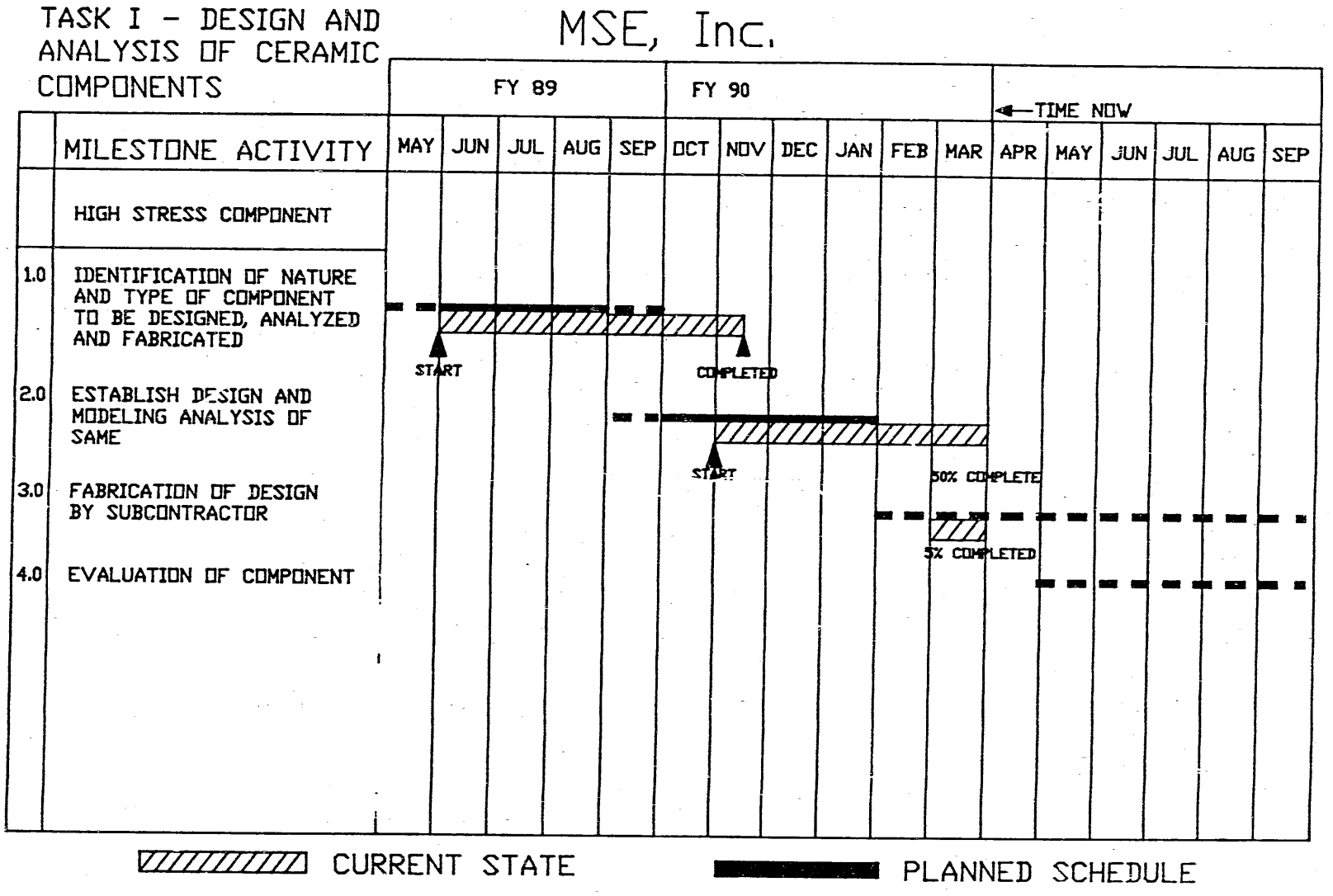
TASK I - DESIGN AND ANALYSIS OF CERAMIC COMPONENTS
MSE, Inc.
FY 89
FY 90
TIME NOW
MILESTONE ACTIVITY
MAY JUN JUL AUG SEP OCT NOV DEC JAN FEB MAR APR MAY JUN JUL AUG SEP
HIGH STRESS COMPONENT
1.0 IDENTIFICATION OF NATURE AND TYPE OF COMPONENT TO BE DESIGNED, ANALYZED AND FABRICATED
START
COMPLETED
2.0 ESTABLISH DESIGN AND MODELING ANALYSIS OF SAME
START
3.0 FABRICATION OF DESIGN BY SUBCONTRACTOR
50% COMPLETE
5% COMPLETED
4.0 EVALUATION OF COMPONENT
CURRENT STATE
PLANNED SCHEDULE

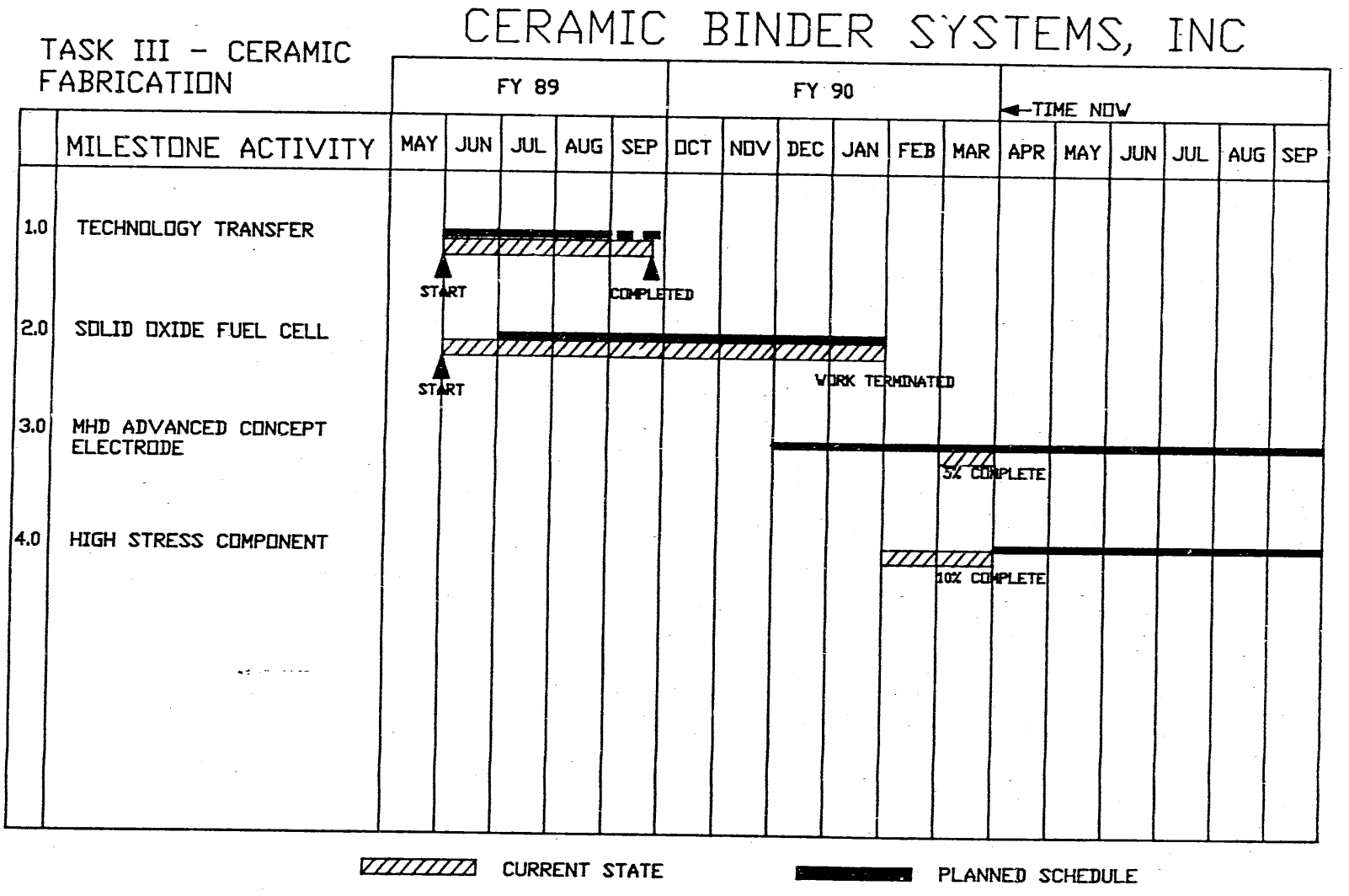
CERAMIC BINDER SYSTEMS, INC
TASK III - CERAMIC FABRICATION
FY 89
FY 90
TIME NOW
MILESTONE ACTIVITY
MAY JUN JUL AUG SEP OCT NOV DEC JAN FEB MAR APR MAY JUN JUL AUG SEP
1.0 TECHNOLOGY TRANSFER
START
COMPLETED
2.0 SOLID OXIDE FUEL CELL
START
WORK TERMINATED
3.0 MHD ADVANCED CONCEPT ELECTRODE
5% COMPLETE
4.0 HIGH STRESS COMPONENT
10% COMPLETE
CURRENT STATE
PLANNED SCHEDULE

CERAMIC R&D FOR DEFENSE APPLICATIONS

DESCRIPTION	FY-89					FY-90											
	MAY	JUN	JUL	AUG	SEP	OCT	NOV	DEC	JAN	FEB	MAR	APR	MAY	JUN	JUL	AUG	SEP
MSE – PROJECTED	5,040	24,480	41,000	68,230	95,170	120,690	145,840	171,040	197,280	222,490	247,990	273,270	298,720	324,000	349,240	374,970	400,000
MSE – ACTUAL	4,800	20,300	34,460	56,203	74,309	90,279	109,486	126,099	145,767	180,242	181,179						
ATL – PROJECTED	600	17,100	55,400	135,600	192,300	239,300	282,600	327,300	378,200	422,400	470,000	515,400	563,000	606,900	654,800	705,700	750,000
ATL – ACTUAL	600	15,573	32,196	67,749	78,847	91,522	132,274	160,636	211,188	247,503	295,977						
CBSi – PROJECTED	940	11,870	30,170	51,590	80,240	103,350	126,460	148,630	174,980	197,820	220,120	242,420	264,180	285,940	307,340	328,670	350,000
CBSi – ACTUAL	940	15,393	37,432	56,074	69,779	81,328	95,975	113,865	140,865	156,803	171,610						
TOTAL – PROJECTED	6,580	53,450	126,570	255,420	367,710	463,340	554,900	646,970	750,460	842,710	938,110	1,031,090	1,125,900	1,218,840	1,311,380	1,409,340	1,500,000
TOTAL – ACTUAL	6,340	51,266	104,088	180,026	222,935	263,129	337,735	400,600	497,820	564,548	648,766						

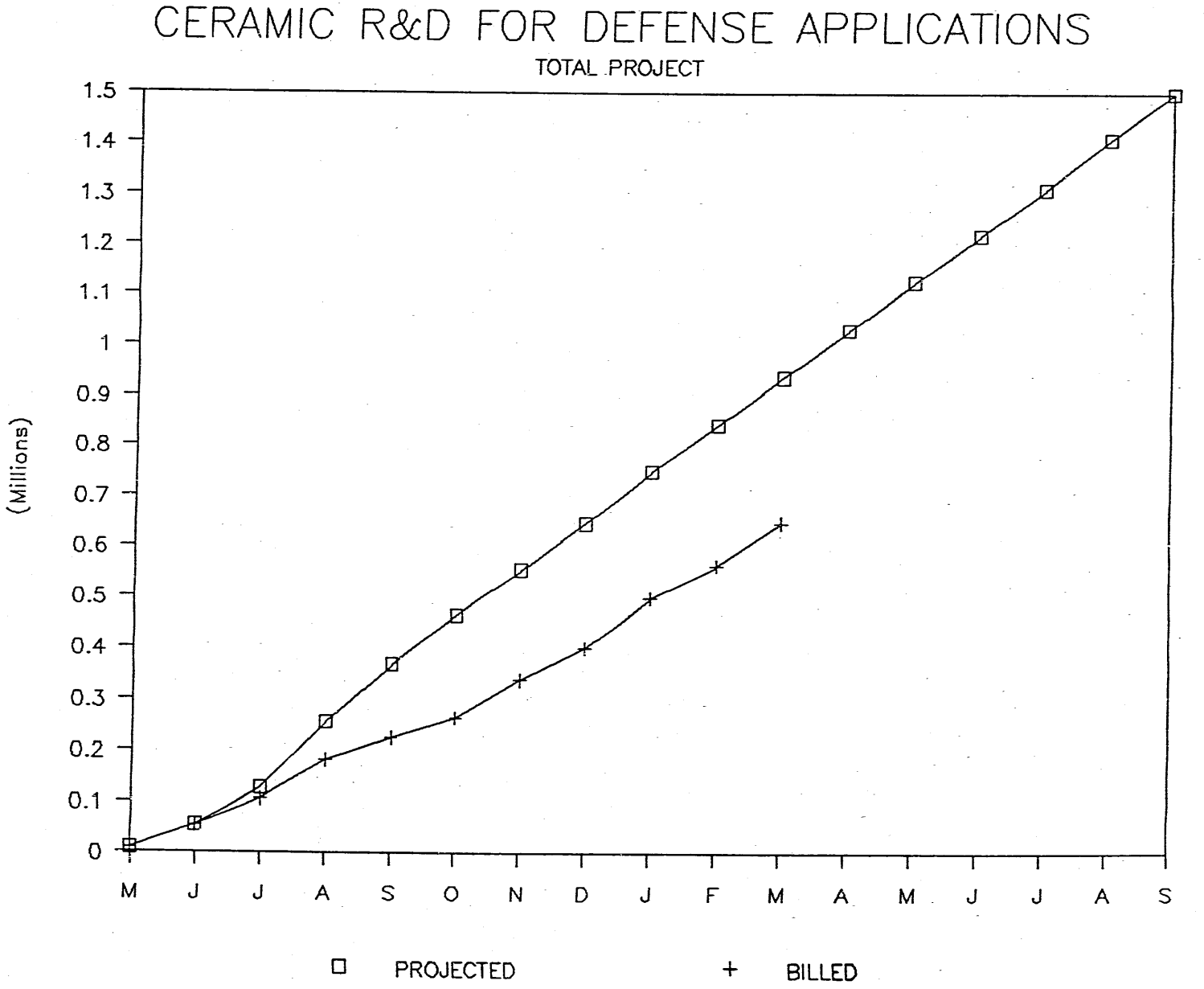
CERAMIC R&D FOR DEFENSE APPLICATIONS
TOTAL PROJECT
(Millions)
1.5
1.4
1.3
1.2
1.1
1
0.9
0.8
0.7
0.6
0.5
0.4
0.3
0.2
0.1
0
M J J A S O N D J F M A M J J A S
PROJECTED
BILLED

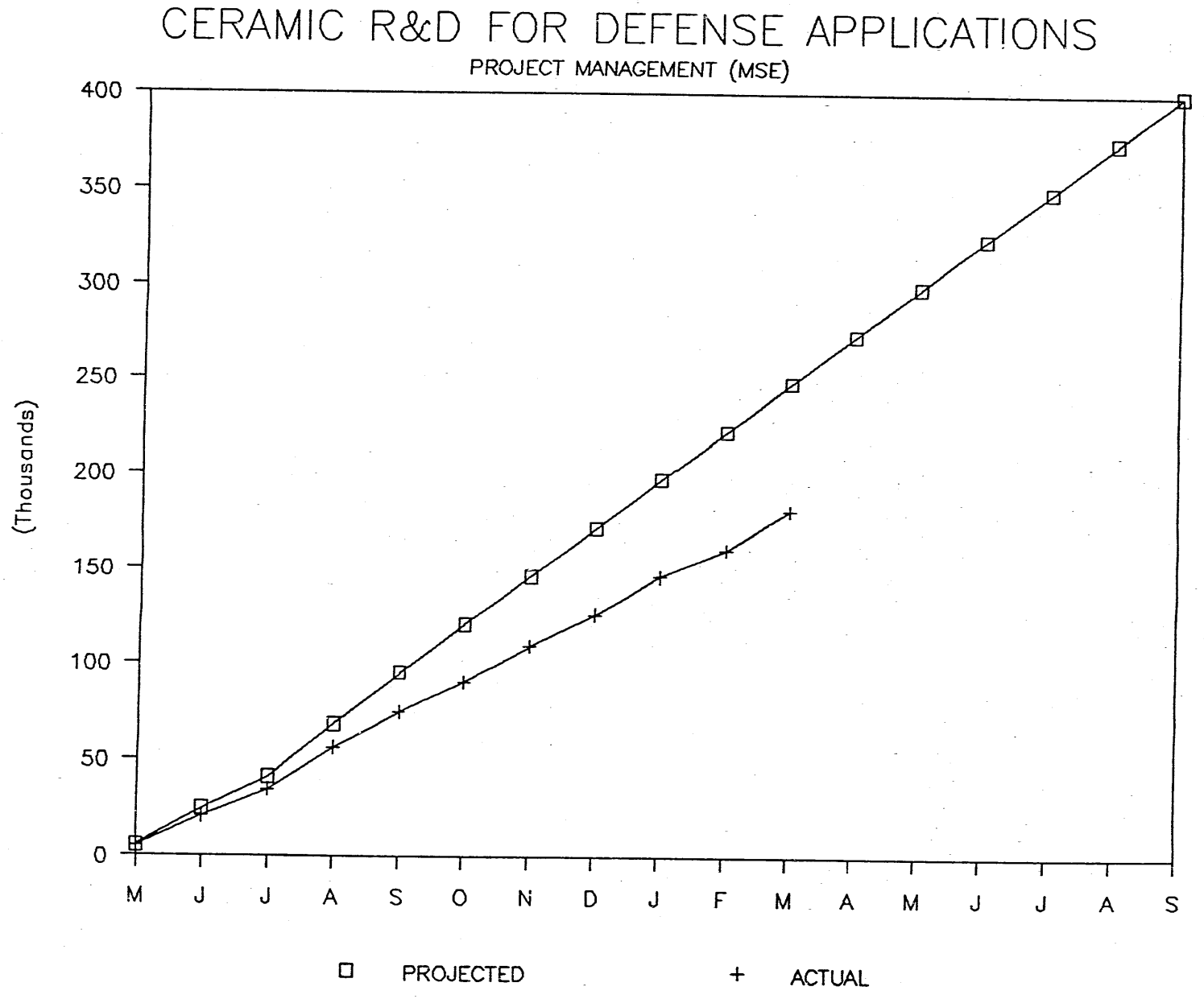
CERAMIC R&D FOR DEFENSE APPLICATIONS
PROJECT MANAGEMENT (MSE)
(Thousands)
400
350
300
250
200
150
100
50
0
M J J A S O N D J F M A M J J A S
PROJECTED
ACTUAL

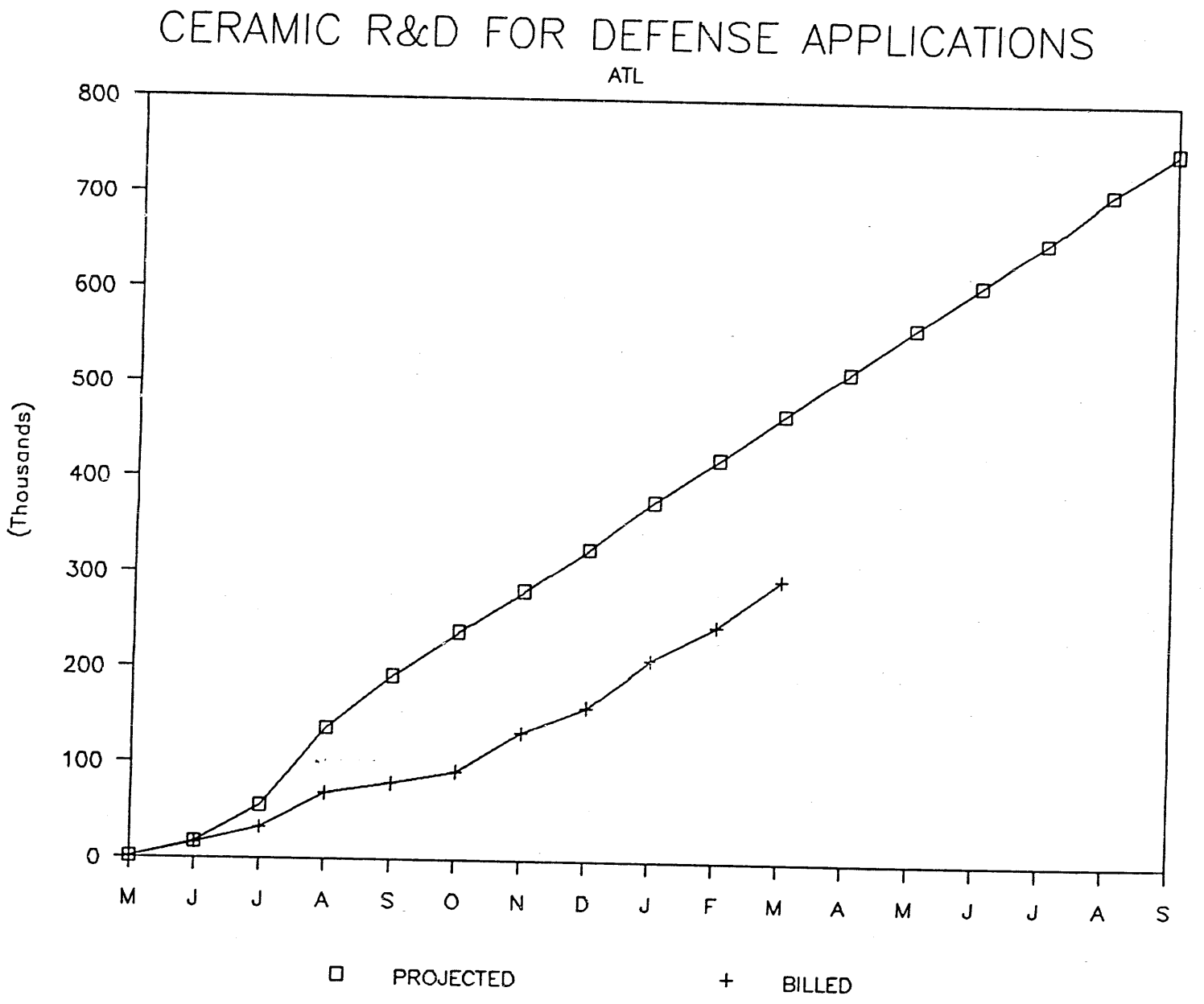
CERAMIC R&D FOR DEFENSE APPLICATIONS
ATL
800
700
600
500
400
300
200
100
0
(Thousands)
M J J A S O N D J F M A M J J A S
PROJECTED
BILLED

CERAMIC R&D FOR DEFENSE APPLICATIONS

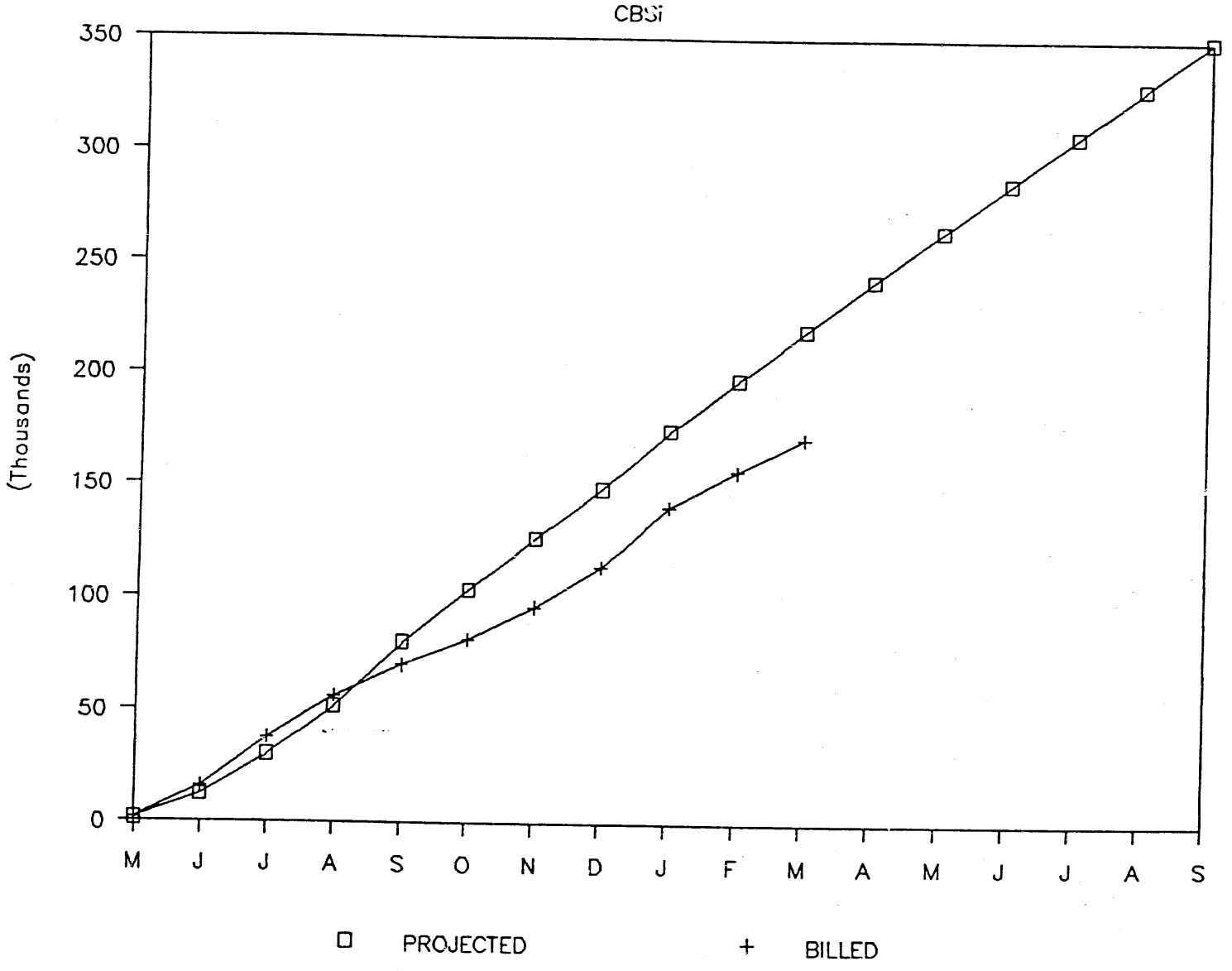

END

DATE FILMED

03/05/91